Doctoral School of Multidisciplinary Medical Sciences
Biochemistry, Biophysics, Molecular and Cell Biology Programme

Albert Szent-Györgyi Medical School

UNIVERSITY OF SZEGED

Ph.D. Thesis

Characterization of the dynamics and mechanism of the nuclear import of Drosophila moesin protein

Zoltán Kovács

Supervisor: Péter VILMOS Ph.D.

HUN-REN Biological Research Centre Szeged

Institute of Genetics

2024.

TABLE OF CONTENTS

PUBLICATIONS

Publications related to the subject of the Ph.D. thesis

I. **Kovács Z.,** Bajusz C., Szabó A., Borkúti P., Vedelek B., Benke R., Lipinszki Z., Kristó I., and Vilmos P. (2024) A bipartite NLS motif mediates the nuclear import of Drosophila moesin. *Frontiers in Cell and Developmental Biology*. 2024 Feb 21;12:1206067. https://doi.org/10.3389/fcell.2024.1206067

IF_{2023}: 6.081, H-INDEX: 87, **Q1**

II. Borkúti P., Kristó I., Szabó A., **Kovács Z.** and Vilmos P. (2024) FERM domain–containing proteins are active components of the cell nucleus. *Life Science Alliance.* 7(4): e202302489. https://doi.org/10.26508%2Flsa.202302489

IF_{2023}: 5.781, **H-INDEX:** 30**, D1**

III. Bajusz C., Kristó I., Abonyi C., Venit T., Vedelek V., Lukácsovich T., Farkas A., Borkúti P., **Kovács Z.,** Bajusz I., Marton A., Vizler Cs, Lipinszki Z., Sinka R., Percipalle P. and Vilmos P. (2021) The nuclear activity of the actin-binding Moesin protein is necessary for gene expression in *Drosophila*. *The FEBS Journal* 288:(16) 4812-4832. https://doi.org/10.1111/febs.15779

IF_{2022}: 4.739, **H-INDEX:** 222, **Q1**

IV. Bajusz C., Kristó I., Borkúti P., **Kovács Z.** & Vilmos P. (2019) Characterization of the nuclear localization signal of the actin-binding Moesin protein. *Biopolymers and Cell* 35(3):201. doi: http://dx.doi.org/10.7124/bc.0009D2

IF: 0.3, **H-INDEX:** 16, **Q4**

Publications not directly related to the Ph.D. thesis

V. Bajusz C, Borkúti P, Kristó I, **Kovács Z,** Abonyi C, Vilmos P. (2018) Nuclear actin: ancient clue to evolution in eukaryotes? *Histochem Cell Biol*. 2018 Sep;150(3):235-244. doi: 10.1007/s00418-018-1693-6.

IF_{2017}: 2.164, **H-INDEX:** 109, **Q1**

VI. Borkúti P, Kristó I, Szabó A, Bajusz C, **Kovács Z,** Réthi-Nagy Z, Lipinszki Z, Lukácsovich T, Bogdan S, Vilmos P. (2022) Parallel import mechanisms ensure the robust nuclear localization of actin in Drosophila. *Front Mol Biosci.* 2022 Aug 19;9:963635. doi: 10.3389/fmolb.2022.963635.
IF$_{2022}$: 6.113, **H-INDEX:** 61, **Q1**

VII. Kristó I, Borkúti P, **Kovács Z,** Szabó A, Szikora S, Vilmos P. Detection of Actin in Nuclear Protein Fraction Isolated from Adult Drosophila Ovary. *Methods Mol Biol.* 2023;2626:353-364. doi: 10.1007/978-1-0716-2970-3_19.
IF$_{2022}$: 1.13, **H-INDEX:** 187, **Q3**

VIII. Szabó A, Borkúti P, **Kovács Z,** Kristó I, Abonyi C, Vilmos P. Measuring Transposable Element Activity in Adult Drosophila Ovaries. *Methods Mol Biol.* 2023;2626:309-321. doi: 10.1007/978-1-0716-2970-3_16.
IF$_{2022}$: 1.13, **H-INDEX:** 187, **Q3**

IX. Borkúti P., Bajusz I., Bajusz C., Kristó I., **Kovács Z.,** Vilmos P. (2019) Testing the biological significance of the nuclear localization of actin. *Biopolymers and Cell* 35(3):204. doi: http://dx.doi.org/10.7124/bc.000A06
IF$_{2019}$: 0.3, **H-INDEX:** 16, **Q4**

X. Kristó I., Bajusz C., Borkúti P., **Kovács Z.,** Pettkó-Szandtner A., Vilmos P. (2019) Investigation the role in mRNA export of the actin binding protein, Moesin. *Biopolymers and Cell* 35(3):219. doi: http://dx.doi.org/10.7124/bc.0009E9
IF$_{2019}$: 0.3, **H-INDEX:** 16, **Q4**

LIST OF ABBREVIATIONS

CDS – Coding sequence

C-ERMAD – C-terminal ERM Association Domain

CRS – Cytoplasmic Retention Signal

dsRNA – double-stranded RNA

ERM – Ezrin-Radixin-Moesin

FDCPs – FERM Domain-Containing Proteins

FERM – 4.1 protein, Ezrin, Radixin, Moesin (domain)

FRAP – Fluorescence Recovery After Photobleaching

HSP – Heat Shock Protein

IκB – nuclear factor of kappa light polypeptide gene enhancer in B cells inhibitor

kDa – kilodalton

LAS AF – Leica Application Suite Advanced Fluorescence

LAS X – Leica Application Suite X (software)

Lat. A – Latrunculin A

MAL – Megakaryocytic Acute Leukemia (protein)

MDCK – Madin-Darby canine kidney (cell line)

Moe – Moesin

moe-GFP – Drosophila moesin tagged with GFP on its C-terminus

N/CP – Nuclear to Cytoplasmic (fluorescence ratio)

NES – Nuclear Export Signal

NF-AT – Nuclear Factor of Activated T cells

NF-κB – nuclear factor kappa-light-chain-enhancer of activated B cells

NLS – Nuclear Localization Signal

NPC – Nuclear Pore Complex

PDB – Protein Data Bank

PIP2 – phosphatidylinositol 4,5-bisphosphate

RNAi – RNA interference

ROI – Region of Interest

SV40 – Simian virus 40

TCR – T Cell Receptor

INTRODUCTION

Evolution of the eukaryotic nucleus and the significance of nucleocytoplasmic transport

Eukaryotes, along with the prokaryotes - Bacteria and Archaea - make up the three domains of life. The main common, unifying feature found in all eukaryotic organisms is the presence of a nucleus, an organelle bound by a double lipid bilayer called the nuclear envelope, whereas in the other two domains there is no such sophisticated compartment. The nucleus' main role is the isolation and containment of the genetic material of the cell, the DNA. With the appearance of the nucleus, the processes of transcription and translation became uncoupled which grants better regulation of gene expression and with it, came many new possibilities for the evolution of eukaryotes, for instance multicellularity (Pennisi, 2004).

There are currently several plausible hypotheses regarding the evolutionary origin of the cell nucleus. One classical theory states that the emergence of the nucleus might be the result of a symbiotic relationship between prokaryotic archaeal and bacterial cells. According to this scenario, an archaeal cell invaded and lived inside of a bacterium. This theory shows analogy to the endosymbiotic origin of the eukaryotic organelles, the mitochondrion and the chloroplast (Martin, 2005). The aforementioned theory belongs to the so-called "outside-in" theories of the origin of the nucleus. As the name shows, these models suggest that the nucleus evolved from the pre-existing endomembrane system which in turn developed from the cell membrane before that (Figure 1).

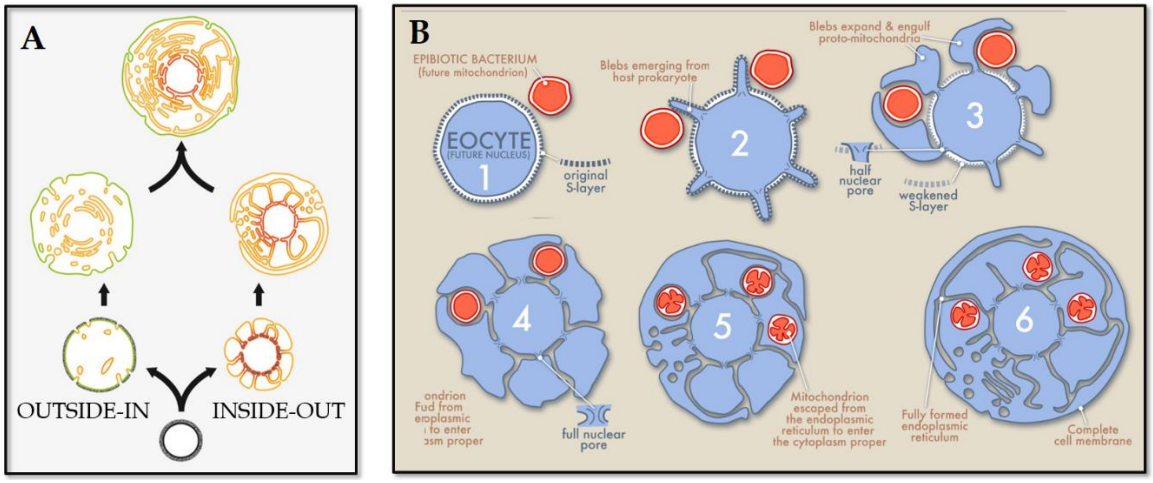

Figure 1. A) Comparison of the outside-in and inside-out theories of nuclear evolution. B) The detailed mechanism of the inside-out origin of the nucleus. Images are based on (Baum, 2015) and (Baum and Baum, 2014), respectively.

Contrary to this, a more recent theory, called the “inside-out” hypothesis states that a prokaryotic cell (the proto-nucleus) grew blebs - protrusions of the cytoplasm - across the cell wall, through which it facilitated material exchange with ectosymbiotic prokaryotes (the proto-mitochondria). The fusion of these blebs around the proto-mitochondria gave rise to the cytoplasm and the continuous spaces between them to the endoplasmic reticulum with the original, protrusion growing cell becoming the nucleus (Baum and Baum, 2014). According to this model, the evolution of endosymbiotic cellular organelles (mitochondria, chloroplasts) and the nucleus took place in parallel, gradually, and does not assume the prior existence of advanced eukaryotic abilities such as for example phagocytosis.

The isolation of the genetic material inside a membrane bound organelle offered many new functions and possibilities that contributed greatly to the evolutionary success of the eukaryotes. Although separated from the rest of the cell, the genome needs a way to maintain connection and communication with its cellular environment in order to function properly. This connection is made possible primarily by the nuclear pore complexes (NPCs). The NPCs are built up of a high number of nucleoporin proteins that form a sophisticated, highly structured protein complex that facilitates membrane transport of various molecules across the nuclear envelope (Devos et al., 2014).

Mechanisms of nuclear transport

Translocation of molecules through the nuclear envelope is possible with two main mechanisms. Small molecules and ions are able to passively diffuse through the NPC, because their small size allows them to pass through in an unrestricted manner. Macromolecules no bigger in size than ~60 kDa are still capable of passive diffusion through the NPCs (Wang and Brattain, 2007). Molecules with molecular weights greater than 60 kDa can enter and exit the nucleus using signal-mediated nuclear transport. This type of nuclear transport requires energy, a nuclear localization signal (NLS) present on the protein in case of import, or a nuclear export signal (NES) for export and a soluble transport machinery that helps facilitating the translocation through the NPC (Kaffman and O’Shea, 1999).

The process of nuclear import has three main steps: docking, translocation through the pore complex and finally, deposition of the cargo in the nucleus (Figure 2). During the first step, the protein to be imported into the nucleus (cargo) is recognized and bound by a soluble import receptor, the importin. The cargo-importin complex is then targeted to the NPC. For the translocation of the cargo-importin complex into the nucleus, the presence of the GDP bound

form of the small GTPase Ran is needed. Inside the nucleus, the cargo-importin complex dissociates by binding of the GTP-loaded form of Ran (Ran-GTP) to the importin. Lastly, the importin gets transported back into the cytoplasm, where it can take part in further cycles of nuclear import (Kaffman and O'Shea, 1999).

The importin recognizes its cargo through a specific sequence of amino acids, called the nuclear localization signal (NLS) which is found on the protein to be imported. Two of the best known NLSs are the simian virus 40 large T-antigen NLS (SV40 NLS) and the bipartite NLS of the protein nucleoplasmin. The monopartite SV40 NLS contains a single, continuous stretch of 7 basic amino acids (SV40 NLS sequence: PKKKRKV). The bipartite NLS of nucleoplasmin is composed of two shorter clusters (2 and 4 amino acids) of basic amino acids separated by a 10 amino acids long spacer (nucleoplasmin NLS sequence: KR[PAATKKAGQA]KKKK, the spacer sequence is between square brackets) (Weis, 1998). But of course, in addition to these classical NLS motifs, numerous forms of nuclear localization sequences have been described today, for a good summary please see for example the recent publication by (Lu et al., 2021).

Regarding its main steps, nuclear export shows similarities to nuclear import. First, the cargo to be exported into the cytoplasm gets recognized through a nuclear export signal (NES) by a soluble export receptor, called an exportin. While alpha and beta importins bind their cargos in the absence of additional proteins, exportins only bind their cargo in the presence of Ran-GTP. The trimeric complex of cargo-exportin-Ran-GTP gets transported through the NPC into the cytoplasm. Once in the cytoplasm, the GTP in Ran-GTP gets hydrolyzed with the help of the Ran-GTPase–Activating Protein (Ran-GAP), therefore becoming Ran-GDP. This change causes the cargo-exportin-Ran-GDP complex to dissociate and the cargo gets released (Figure 2) (Mattaj and Englmeier, 1998). The best known nuclear export pathway uses a leucine-rich nuclear export signal which is recognized by the nuclear export receptor Crm1 (also known as Exportin1) (Fornerod et al., 1997).

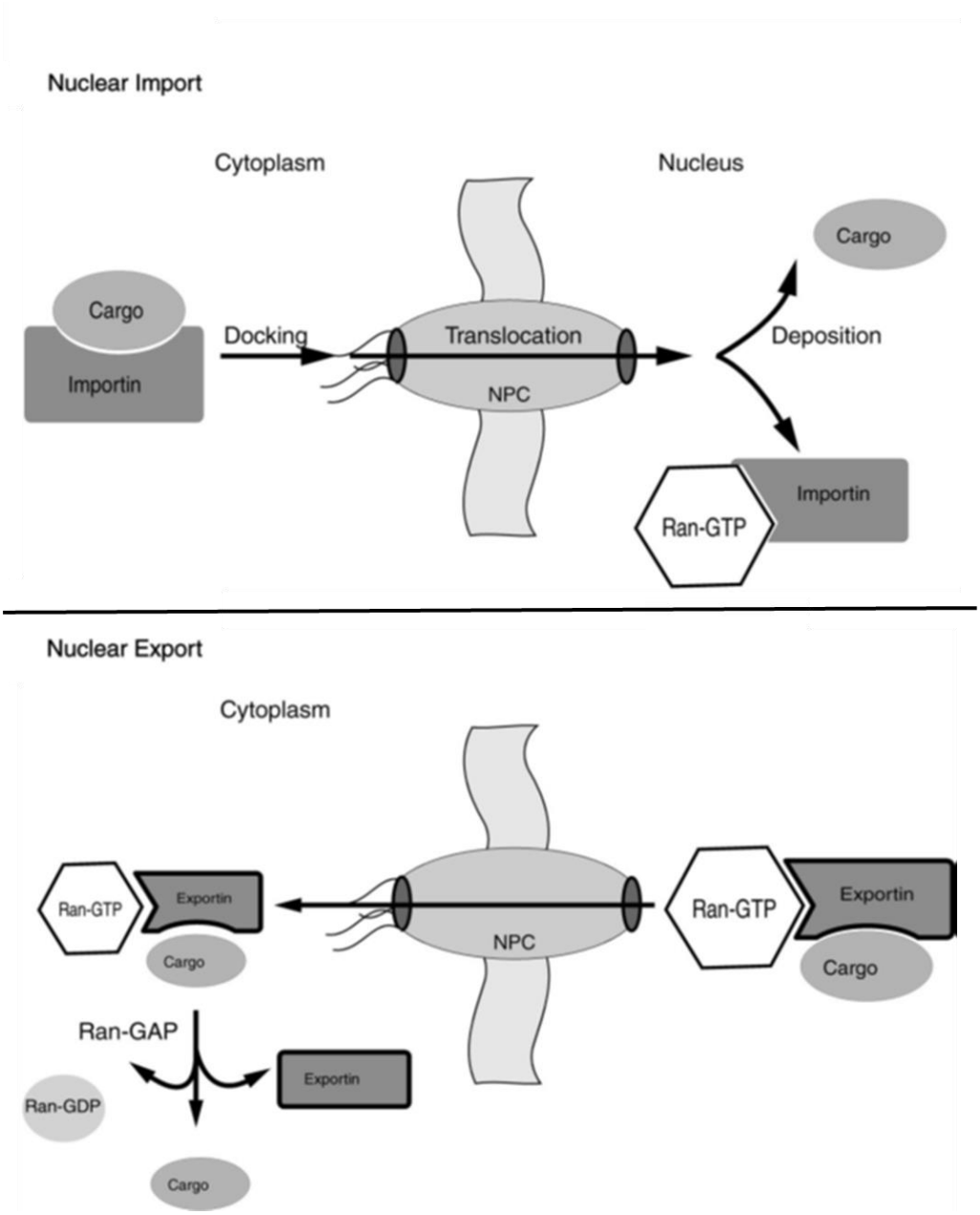

Figure 2. Main steps of nuclear transport. Figure is based on Kaffman and O'Shea, 1999, Figure 1.

Regulation of subcellular localization

NLS and NES sequences can target proteins to either the nucleus or the cytoplasm, but the regulation of the subcellular localization of proteins have a few more ways that fine tune their distribution. Among these regulatory mechanisms is the post-translational modification of the cargo which can prevent or promote the formation of the cargo-transport receptor complex. Similarly, the activity of the transport receptor can also be altered to influence complex formation with the cargo. If the cargo-transport receptor complex is already formed, then it could be anchored to an insoluble component, therefore preventing interaction of the complex

with the NPC. Another possible step of regulation is the modification of the NPC itself which could affect the properties of the transport (Kaffman and O'Shea, 1999; Hung and Link, 2011).

An example for the regulation of subcellular localization by phosphorylation is the case of the nuclear factor of activated T cells (NF-AT) proteins. Members of the NF-AT protein family are transcription factors that play an important role in the immune response upon stimulation of the T cell receptor (TCR). Under uninduced conditions, NF-AT is phosphorylated and can be found in the cytoplasm in a conformation, in which the NES is accessible, but the NLS is not. Upon TCR activation, cytosolic calcium levels rise, activating the phosphatase calcineurin. Calcineurin binds to NF-AT, masking the NES and quickly dephosphorylates it, causing a conformational change in NF-AT which exposes the NLS. This complex of calcineurin-NF-AT gets imported into the nucleus, where NF-AT can take part in transcription (Shibasaki et al., 1996). If the calcium level drops, the calcineurin-NF-AT complex dissociates, kinases inside the nucleus phosphorylate NF-AT which causes it to revert back to a conformation, in which the NLS is not accessible, but the NES is which is then recognized by the exportin Crm1, and the complex gets exported into the cytoplasm (Zhu and McKeon, 1999).

The formation of intermolecular complexes is another way by which nuclear localization can be achieved or inhibited. In the case of nuclear factor kappa-light-chain-enhancer of activated B cells (NF-κB), association with another protein causes its retention in the cytoplasm. The NF-κB protein family members share an N-terminal Rel homology domain which is responsible for DNA binding, dimerization and also serve as a recognition site for the regulatory protein nuclear factor of kappa light polypeptide gene enhancer in B cells inhibitor (IκB). The NF-κB dimeric proteins are activated by multiple stimuli and in response to them, translocate to the nucleus and induce the transcription of multiple genes that play important roles in immune response. Without a stimulus, the NF-κB dimers can be found in the cytoplasm, bound by IκB. IκB retains NF-κB in the cytoplasm and in an inactive state by multiple measures. The bound IκB masks the NLS of NF-κB, therefore preventing its nuclear entry, but promotes its nuclear export (Arenzana-Seisdedos et al., 1997) and also inhibits its DNA binding activity (Baeuerle and Baltimore, 1988). The appropriate stimulus activates a kinase that phosphorylates IκB and targets it for degradation. With the degradation of IκB, NF-κB through its now accessible NLS quickly translocates into the nucleus and takes part in the transcriptional response to the stimulus (Rothwarf et al., 1998).

The nuclear factor 7 (Xnf7) protein of the African clawed frog, *Xenopus laevis* is a maternally expressed transcription factor that has important role in the determination of the dorsal-ventral body axis of the developing frog embryo. Xnf7 is retained in the cytoplasm of the oocyte up until the midblastula transition phase of development, during which it translocates into the nucleus. This retention in the cytoplasm is achieved by a 22 amino acids long cytoplasmic retention domain (CRD) that acts in cooperation with two phosphorylation sites. Unlike in the case of the previously mentioned protein, NF-κB, Xnf7's cytoplasmic retention does not work by masking of the NLS, because fusion of an extra NLS to the C-terminus of the protein did not disturb cytoplasmic retention in any way. Further supporting the notion of a dedicated cytoplasmic retention site, deletion of the CRD resulted in premature nuclear entry of Xnf7 (Li et al., 1994).

The retention of proteins in the cytoplasm can be performed by many binding partners or even heat shock proteins, but there are also factors that specialize in this activity. Proteins in the 14-3-3 family are such a group of evolutionary conserved regulatory molecules. One of their most interesting features is the ability to bind and sequester a plethora of functionally diverse molecules in the cytoplasm, including transmembrane receptors, phosphatases and kinases. So far, more than 200 molecules have been shown to act as substrates for 14-3-3 proteins. With this wide range of partners, 14-3-3 proteins play important roles as regulators of cellular functions such as cell cycle control, signal transduction and apoptotic cell death. 14-3-3 proteins recognize their substrates through two main ways. Usually, 14-3-3 proteins interact with their regulated partners through a phosphoserine-containing consensus motif, that is, RSxpSxP, where "pS" is phosphoserine and "x" represents any amino acid. Although in most of the cases interaction is mediated through this motif, there are known examples, in which 14-3-3 recognizes an unphosphorylated ligand. In the case of Raf-1, a serine-threonine protein kinase, there is a cysteine-rich 14-3-3 recognition site on the protein that contains no phosphorylatable amino acids, yet it was still able to interact with 14-3-3 *in vitro*. Other examples of unphosphorylated 14-3-3 ligands include for example the ExoS ADP-ribosyltransferases and the 43 kDa inositol polyphosphate 5-phosphatase (Fu et al., 2000).

The ERM protein family

During my PhD studies I investigated the nuclear import mechanism of the Drosophila moesin protein belonging to the evolutionary conserved ERM protein family which consists of three paralogs in vertebrates: ezrin, radixin and moesin. The three members of the family show

somewhat different expression patterns, for example, epithelial cells are predominantly expressing ezrin, while endothelial cells tend to express mostly moesin. Non-vertebrate species have only one ERM protein coding gene. In the case of *Drosophila melanogaster*, the single ERM protein coding gene is called *moesin*.

ERM proteins display a high degree of structural similarity to each other. They have three distinct domains, an N-terminal, globular FERM (abbreviated form the names Band 4.1, **E**zrin, **R**adixin, **M**oesin) domain, the so called C-ERMAD (C-terminal ERM Association Domain) at the C-terminus, and a flexible alpha-helical domain which connects the two. The FERM domain is about 300 amino acids long and can be further divided into three subdomains: F1, F2 and F3 which are arranged like the leaves of a clover. The FERM domain, being a versatile protein binding domain, is responsible for the interaction with numerous membrane associated proteins. The C-terminal domain has two major functions. It is the site of F-actin binding, and secondly, it plays role in the regulation of the ERM protein itself by being able to both inter- and intramolecularly bind the FERM domain. This inactivation through self-binding is facilitated by the flexion of the middle, alpha-helical domain (Figure 3) (Fehon et al., 2010).

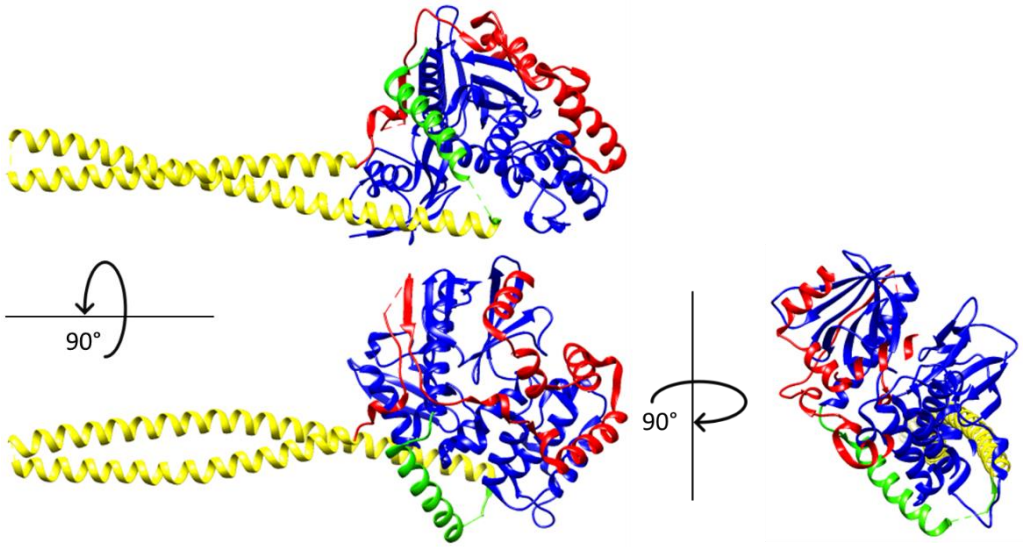

Figure 3. Structure of full-length, closed conformation *Spodoptera frugiperda* moesin. FERM domain is highlighted in blue, the C-terminal actin binding domain is red. The flexible alpha-helix connecting the two terminal domains is shown in yellow. Green indicates a short alpha-helix connecting the FERM and the alpha-helical domains. PDB ID: 2I1K

The activity of the ERM proteins is regulated through head-to-tail folding because in their closed state, when the C-ERMAD is bound to the FERM domain, the intramolecular interaction masks the binding sites on the surface of the FERM domain. In order to achieve an open, active

conformation, ERMs must bind phosphatidylinositol 4,5-bisphosphate (PIP2) on a specific binding pocket located on the FERM domain which in turn causes the incomplete opening of the molecule. In this partially opened state, a threonine residue in the C-ERMAD becomes accessible and gets phosphorylated which causes the full and stable opening of the molecule (Nakamura et al., 1995; Fievet et al., 2004; Ben-Aissa et al., 2012).

Classically, ERM proteins act as crosslinkers between integral membrane proteins and the actin cytoskeleton, playing a structural and membrane organizing role. Membrane protein interactors of the ERMs include for example the CD43, CD44 and ICAM-1, -2, -3 molecules. Given the ability of ERMs to facilitate interactions between multiple proteins at the cell cortex, they are also suitable for the control of signal transduction pathways. RhoA is a small GTPase protein that plays a role in regulating the cortical actin cytoskeleton. Through interaction with downstream effectors, RhoA takes part in cellular processes such as morphogenesis, cytokinesis and cell migration (Fehon et al., 2010). In *Drosophila melanogaster*, it has been shown that moesin negatively regulates Rho1, the fly orthologue of RhoA (Speck et al., 2003). In a study conducted with the help of the popular model organism *Drosophila melanogaster* using hypomorphic *moesin* alleles it was found that out of the main signaling pathways that are known to function in wing development (*notch*, *wingless*, *decapentaplegic*, *EGFR* and *hedgehog*) only *hedgehog* was affected by the *moesin* mutation. Hedgehog targets that require high levels of signaling output were affected, suggesting that moesin plays a role in hedgehog signaling (Molnar and de Celis, 2006).

ERM proteins in the nucleus

With new results emerging, today it is clear that the majority of cytoskeletal proteins is present not only in the cytoplasm, where they perform their classical, well known tasks, but also in the nucleus. Because of its abundance, essential functions and evolutionary conservation, one of the best known cytoskeletal proteins, actin was extensively studied from the very beginning, but research almost exclusively focused on its cytoplasmic activities. Although actin was reported to be present in the nucleus already in the 1960s, for a long time this observation was received with skepticism. Today we know that actin plays important roles in the nucleus, by taking part in processes which regulate the activity of RNA polymerases and transcription factors, chromatin remodeling complexes and histone deacetylases. Nuclear actin also contributes to human diseases, such as cancer, neurodegeneration and myopathies. Today

it is also known that the nuclear transport of actin, due to its essential nuclear functions, is a tightly regulated, active process (Dopie et al., 2012; Kelpsch and Tootle, 2018).

Like actin, many cytoskeletal proteins also localize in the nucleus, including FERM-domain-containing proteins (FDCPs), one of whose representatives is investigated in our laboratory. FDCPs evolved at the dawn of eukaryotes, when plants and Amorphea (amoebas, fungi and animals) separated, about 1.4 billion years ago (Ali and Khan, 2014), long after the development of the cell nucleus. Despite this and their primarily cytoplasmic functions, almost all members of the FDCP family have been detected in the nucleus, in fact there is a strictly regulated amount of them in the nucleus which is in dynamic equilibrium with their cytoplasmic pool. In some cases, the family's ancient, highly conserved FERM domain contains the NLS motif that controls entry into the nucleus, but the location and sequence of the nuclear localization signal still show extremely high diversity among FDCPs (Figure 4). This variability in the nuclear transport and also functions of different FERM domain proteins that appeared at different points in the evolution provides the obvious conclusion that the nucleus of eukaryotes evolved and continues to evolve as continuously as the whole cell or even the multicellular organisms made up of it.

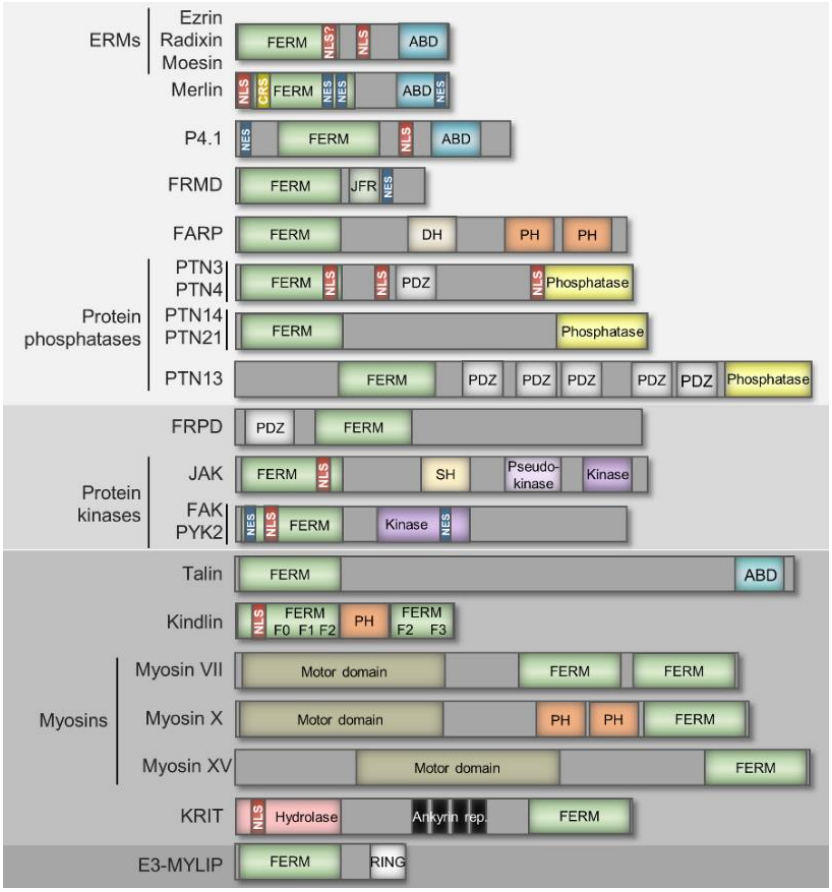

Figure 4. Domain structure of FDCPs. Proteins are grouped according to the phylogenetic relations of the FERM domains (Ali and Khan, 2014). Only most relevant domains are shown, size is not for scale. Structures are shown in N- to C-terminal direction. Known NLS, NES and CRS motifs are highlighted with red, dark blue and yellow rectangles, respectively.

Similar to actin and the other FDCP proteins, the presence of ERM proteins in the nucleus has been also reported (Figure 5). Among the earliest observations of this phenomenon was when a 55 kDa, endogenously cleaved fragment of ezrin was shown to localize to the nucleus (more specifically, to the nucleolus) in human cells (Kaul et al., 1999), or when full length ezrin was observed by immunofluorescence in the nuclei of rat Schwann cells (Melendez-Vasquez et al., 2001). Later, by 2D-gel electrophoresis and subsequent mass spectrometry analysis moesin was also detected in the nuclei of human lymphocytes (Bergquist et al., 2001). In MDCK (Madin-Darby canine kidney) cells the amount of nuclear ezrin and moesin was found to depend on cell culture density. The nuclear localization of the proteins was much more prominent is subconfluent cell cultures than in confluent ones. It was also shown that exogenously expressed, GFP-tagged radixin, the last member of the ERM family, of which so far we haven't talked much about, also localizes to the nucleus. Differential detergent extraction experiments revealed that ezrin and moesin are tightly associated with nuclear components which further supports the notion that there are certain nuclear functions, for which ERM proteins can be found in the nucleus (Batchelor et al., 2004).

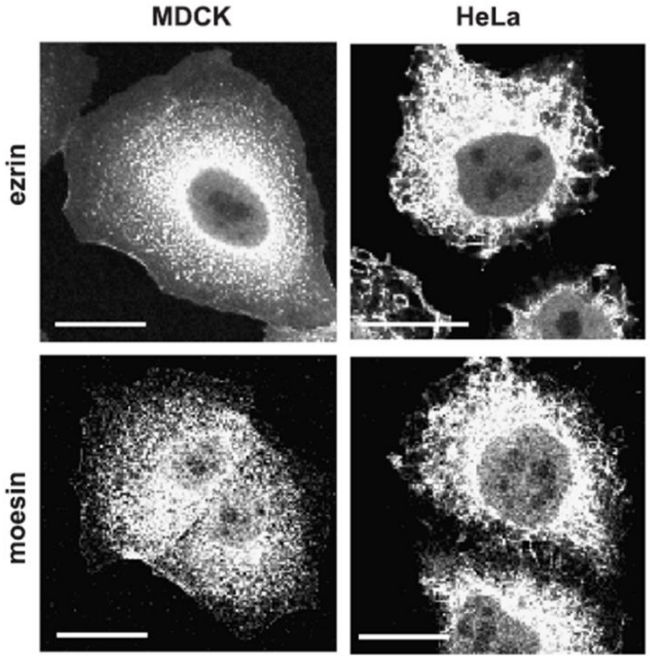

Figure 5. Ezrin and moesin are present in the nucleus of canine (MDCK) and human (HeLa) cells. Scale bars: 20 μm. Source: Batchelor et al., 2004, Figure 1.

The Drosophila ERM protein, moesin in the nucleus

In vertebrates, the functional redundancy posed by the simultaneous presence of the three family members hinders the study of ERM proteins. Fortunately, in the well-established model organism, *Drosophila melanogaster*, there is only a single representative of the family, the Drosophila moesin protein. Like its vertebrate homologs, Drosophila moesin has been shown to localize not just in the cytoplasm, but also in the nucleus. It was shown in cultured Drosophila S2 cells and embryos that moesin localizes to the nucleus in interphase, and that it shows a nuclear distribution complementary to the chromatin. Upon entering prophase, the amount of nuclear moesin rapidly increases. During meta-, ana- and telophases, the protein shows a localization complementary to the chromosomes and it co-localizes with the mitotic spindle, suggesting a direct role in mitosis (Vilmos et al., 2009).

Later studies in the fruit fly shed more light on the nuclear functions of moesin. Upon blocking the nuclear export of mRNAs by knocking down mRNA export factors, such as Nup98 or Rae1, moesin accumulates to high levels in the nucleus. Using the polytene chromosomes of the Drosophila larval salivary gland, it was shown that moesin localizes to the chromosome puffs which are special euchromatic regions with extremely high transcriptional activity. Chromosome puffs form as a result of certain stimuli, for example heat-shock or hormone treatment. Using these stimuli, the authors showed that the respective puffs formed on the chromosomes and that moesin localized to them. The authors also demonstrated that moesin is a constituent of the mRNP particles which are responsible for the nuclear export of mRNAs, suggesting that the protein plays role in mRNA export as well (Kristó et al., 2017).

The biological significance of nuclear moesin was examined in *Drosophila* (Bajusz et al., 2021). Since the complete absence of moesin activity is lethal for the cell, and also because any change in the protein would affect not only its nuclear, but its essential cytoplasmic functions as well, the authors created a version of moesin in fruit flies that is fused with a nuclear export signal (NES). This moesin-NES protein constantly gets exported out of the nucleus, therefore significantly lowering the nuclear levels of moesin, even in situations, in which the amount of the protein should be increased. While the cytoplasmic activity and function of moesin-NES proved to be unchanged, various phenotypes could be observed as a consequence of the disturbance of the nuclear pool. Flies expressing the moesin-NES mutant protein exhibited slow development, decreased lifespan, egg production and climbing ability, and genitalia rotation in males. The consequences of reduced nuclear moesin levels were evaluated also at the molecular level by an mRNA-Seq analysis. The experiment revealed that the expression of 371 genes

were up- and 315 were downregulated (Bajusz et al., 2021). Among the upregulated genes were three important players in development: *vasa*, *Notch* and *dpp*. This could help explain the developmental defects observed in the moesin-NES mutant animals. Another interesting group of genes that were downregulated in moesin-NES animals were Heat shock protein (HSP) encoding genes, namely *hsp70Aa, hsp70Ab, hsp70Ba, hsp68, hsp26,* and *hsp23*. This result is in concert with the findings published earlier (Kristó et al., 2017), where upon heat-shock, moesin localized to the heat shock puffs on polytene chromosomes in Drosophila larval salivary glands, indicating that moesin is required for the transcription of heat-shock genes.

AIMS

Actin-binding FERM domain-containing proteins were already observed to be present in the cell nucleus decades ago, and in the case of some of them, the nuclear functions have also been described in sufficient details. However, the mechanism and regulation of their nuclear transport, even in the case of the best characterized proteins, is still barely known. This is despite the fact that the exploration of nuclear transport can be of great help both in understanding the nuclear function of a given protein as well as in manipulating it. In the present study, we aimed to answer the following questions:

1. What is the dynamics of the nuclear import of moesin?
2. Is the bipartite NLS of moesin evolutionarily conserved? Does conservation reveal other properties of the NLS, such as its regulation?
3. Does phosphorylation play a role in the regulation of the nuclear import of moesin?
4. Can open or closed conformation regulate moesin's import?
5. What other mechanisms regulate the nuclear import of moesin?

MATERIALS AND METHODS

Molecular cloning and DNA constructs

Coding sequences (CDS) of different proteins were amplified using PCR primers with Gateway BP adapter sequences from clones from the Drosophila Gold Collection (Berkeley Drosophila Genome Project). Next, the amplicons were used in Gateway BP recombination reactions (Invitrogen, Gateway BP Clonase II Enzyme Mix, 11789) with the Gateway pDONR221 vector in order to generate an entry clone. From this entry clone, the CDS of the protein of interest could be cloned with the Gateway LR reaction (Invitrogen, Gateway LR Clonase II Enzyme Mix, 11791) into a Gateway expression vector, from which the cells were able to produce the protein of interest as a fusion protein (e.g.: tagged with GFP) after transfection. Gateway cloning steps were carried out according to the instructions of the manufacturer.

Mutant forms of moesin carrying either point mutations (e.g.: MoeT559A, MoeY292E) or deletions of various sizes (e.g.: MoeΔCRS) were created using the Q5 Site-Directed Mutagenesis Kit (New England Biolabs, Cat. No.: E0554S), following the instructions of the manufacturer.

The CRS-tags were designed to function as short peptide tags fused to the C-terminus of GFP. The basis for the creation of these constructs was the N-terminally GFP-tagging Gateway expression plasmid, pAGW, with short inserts cloned into the vector acting as the tags of GFP. Various dsDNA strands containing the coding sequences of the CRS tags were generated using PCR with Gateway adapters on their 5’ and 3’ ends. These inserts were cloned into pAGW with the Gateway BP cloning reaction. In the case of the control construct expressing only GFP, the insert contained a STOP codon right at its beginning, therefore terminating translation right after GFP. The insert of the control construct GFP-R60 was based on a randomly selected 180 base pairs long stretch of the CDS of Actin5C. This part was amplified with a 5’ primer designed to introduce a frameshift, therefore resulting in an insert that coded for random 60 amino acids. The rest of the CRS-tags (CoreCRS, CRS, Exon10) were amplified from the Moe-pDONR221 construct with the appropriately designed primers.

Cell culturing

Drosophila S2R+ cells were cultured at 25°C in a Memmert IPP110 incubator in Schneider’s Drosophila Medium (Biowest, L0207-500) supplemented with 10% Fetal Bovine Serum (Biowest, S1820-500) and 1% Penicillin/Streptomycin (Capricorn Scientific, PS-B),

using 25 cm^2 cell culture flasks (VWR, 10062-872). Upon reaching confluence, the cells were trypsinized using Trypsin-EDTA (Capricorn Scientific, TRY-1B) and transferred into a new cell culture flask.

Transient transfection of cells

For live cell experiments, cells were seeded in 35 mm glass-bottom Petri dishes (Cell E&G, GBD00001-200). The cells were then transfected using the jetOPTIMUS transfection reagent (Polyplus, 101000006), according to the manufacturer's instructions. For experiments without RNAi, $10x10^5$ cells were seeded and they were examined on the second day post-transfection. When RNAi was used, $6x10^5$ cells were seeded and examined on the fifth day after transfection.

For immunostaining experiments, round, 12 mm in diameter cover slips (Epredia, CB00120RA120MNZ0) were placed onto the bottom of wells of 24-well plates (SPL Life Sciences, 32024). The cells were seeded onto the cover slips in the wells, $130x10^3$ cells per well and transfected with the jetOPTIMUS transfection reagent, as described in the previous paragraph. Cells were grown in these plates for five days before immunostaining.

RNA interference

Target sequence identification and primer design for RNA interference were carried out with the help of SnapDragon (https://www.flyrnai.org/snapdragon). RNAi target sites were amplified in a PCR reaction, with primers designed to carry T7 promoter sequences on their 5' ends. With the PCR product as template, in vitro transcription reactions were set up to produce the dsRNA for the RNAi experiments. For the in vitro transcription reactions, the Invitrogen MEGAscript T7 High Yield Transcription Kit (Invitrogen, AM1334) was used. The product of the in vitro transcription reaction was purified using the Zymo Research Quick-RNA MiniPrep kit (Zymo Research, R1054).

The RNAi construct for the knock-down of *Rae1* was designed earlier by my colleague, Ildikó Kristó, using the method described above.

Double stranded RNAs were transfected along with the plasmids coding for the GFP-tagged version of the protein of interest, in one transfection reaction. In order for the RNAi to exert its effect, we had to wait five days after transfection.

Chemical treatment of cells

Jasplakinolide desiccate (Invitrogen, J7473) was dissolved in DMSO in order to produce a stock solution of 1mM. Two hours prior to immunostaining, cells were treated with Jasplakinolide in a final concentration of 5 μM. For Latrunculin A treatment cells were incubated for 20 minutes with either Latrunculin A (Sigma-Aldrich, L5163-100UG) at a final concentration of 5 μM, or an equal volume of its solvent DMSO (Sigma-Aldrich, 589569) as a control on the fifth day after transfection.

Immunostaining of S2R+ cells

Transfected cells adhered to round glass coverslips were washed 1x with PBS, fixed in 4% PFA-PBS for 20 minutes at room temperature, then washed 3x 2 minutes in PBS. Fixed cells were permeabilized with PBT (PBS + 0.1% Triton X-100) for 5 minutes. Non-specific reactions were blocked with PBT-N solution (PBT, 1% BSA, 5% FCS) for 1 hour. Samples were incubated overnight (O/N) with rabbit polyclonal anti-GFP (1:500, Thermo Fisher Scientific, A-6455) primary antibody at 4°C. Next day the samples were washed 3x 2 minutes with PBS and incubated with the fluorescently labeled secondary goat anti-rabbit Alexa Fluor 488 antibody (1:500, Thermo Fisher Scientific, A-11008) for 1 hour at room temperature in dark. After washing 3x with PBS, DAPI (0.2 μg/ml, Sigma-Aldrich, D9542) in PBT-N was applied for 1 h in dark at room temperature. In the case of experiments, where Phalloidin staining was also used, Phalloidin Alexa Fluor 546 (1:40, Thermo Fisher Scientific, A22283) was employed along with DAPI in PBT-N. Samples were washed 3x in PBS, and the coverslips were placed upside down in a drop of mounting medium (Fluoromount G, Thermo Fisher Scientific, 00-4958-02) on a microscope slide.

Microscopy

For the microscopy experiments a Leica TCS SP5 confocal microscope was used with a 63x oil immersion, NA1.4 objective and Leica Application Suite Advanced Fluorescence (LAS AF) software.

FRAP experiments

FRAP experiments were carried out with the help of the FRAP Wizard function of the LAS AF software. During a nuclear FRAP assay, 5 pre-bleach images were taken of the whole unbleached cell in the beginning, followed by 2-5 bleaching scans with high laser intensity,

focused on the nucleus. For the recording of the recovery, the whole cell was monitored for the rest of the experiment, creating a Z-stack of 10 slices every minute. The distance between the slices of the stack was 1 μm. Using Z-stacks was a way to compensate for the movement of the living cell and to keep the nuclear middle plane in focus during the whole timeframe of the experiment.

In the case of the cortical FRAP experiments, a short section of the cell cortex was selected as the target of the photobleaching. Five pre-bleach images of the whole cell were taken, then 2-5 bleaching scans were used on the designated Region of Interest (ROI), followed by scans of the whole cell, taking one every ~1,3 seconds for 4 minutes. "Blind FRAP" experiments were performed to explore the magnitude of unwanted bleaching caused by the scanning of the cell after the bleaching event during a long nuclear FRAP assay. The "blind FRAP" assays were carried out exactly as described in the "FRAP experiments" part above, but in this case, the laser intensity was reduced to zero during the bleaching scans, therefore no intentional photobleaching was introduced. With the data points calculated from measured pixel intensity values (explained in detail in the "Data analysis and statistics" paragraph of Materials and Methods), we created graphs depicting the FRAP curves (Figure 6).

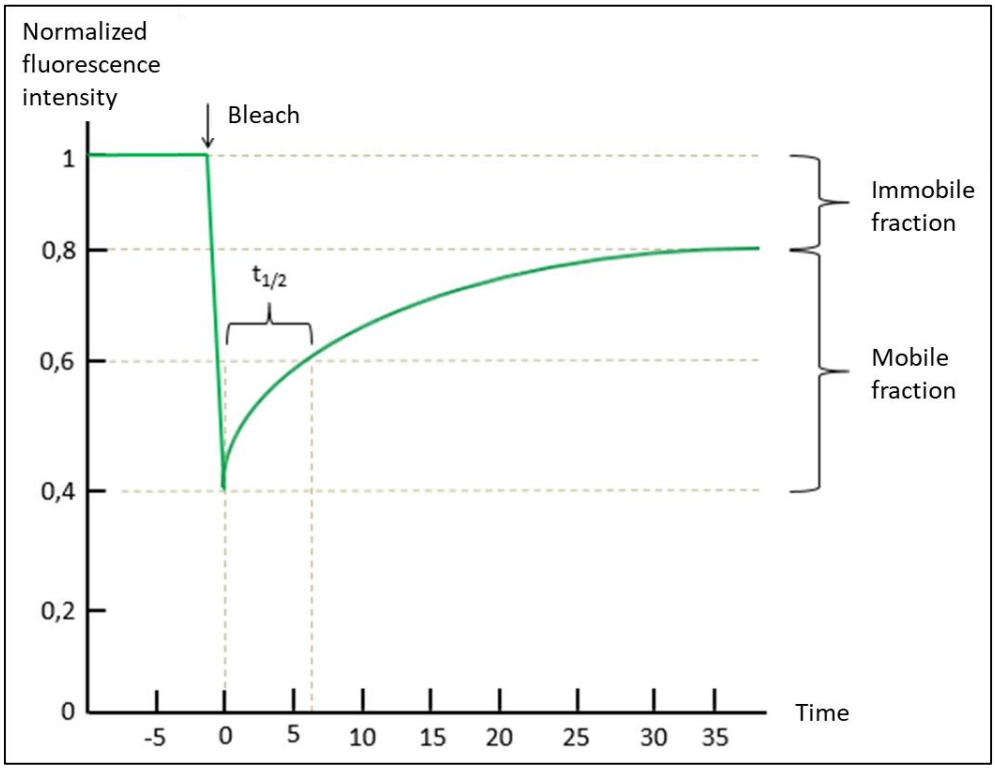

Figure 6. Schematic of an ideal FRAP curve, with data describing the mobility of the protein of interest ($t_{1/2}$, Immobile and mobile fractions) indicated.

Data analysis and statistics

Photos taken with the microscope were exported as .tiff files using the Leica Application Suite X (LAS X) software. Mean pixel intensity values were measured in the images with the help of ImageJ. In the images taken during the FRAP experiments, the average pixel intensity values were measured at three locations per cell: in the nucleus, in the cytoplasm, and in an area outside the cell where only background fluorescence could be observed. Background corrected nuclear to cytoplasmic fluorescence ratios (N/CP ratios) were calculated in Microsoft Office Excel 2016 with the formula: (N-BG)/(CP-BG), where N: nuclear, CP: cytoplasmic and BG: background mean pixel intensities. In the images of fixed, immunostained cells the nuclear and cytoplasmic mean pixel intensities were measured to calculate the nuclear to cytoplasmic fluorescence ratio using the formula: N/CP, where N: nuclear, CP: cytoplasmic mean pixel intensities.

Statistical analysis of data gathered and calculated were performed using the Analysis ToolPak add-in of Microsoft Office Excel 2016, GraphPad Prism 9 software and the R programming language. For pairwise comparisons, first, data sets were evaluated for the normality of the distribution of data points. Based on normality, the appropriate nonparametric (Mann-Whitney U test) or parametric (Student's t-test) test was used.

In the case of the experiment depicted by Figure 15, two-way ANOVA was performed to analyze the *Rae1* and *Slik* RNAi effect on the nuclear and cytoplasmic distribution of GFP signal.

The graphs showing FRAP curves and N/CP ratios were created with the help of the GraphPad Prism 9 software. Curve fittings on the FRAP graphs were also carried out in GraphPad Prism 9 using the "One phase decay" equation (nonlinear regression). For the quantification of the immunostaining experiments, 25-25 cells from 3 technical repetitions, i.e. a total of 75 data per sample, were analyzed and plotted. Statistical significance indicated in the graphs is marked with ***: $p < 0.001$, **: $p < 0.01$, *: $p < 0.05$, and n.s. (not significant): $p > 0.05$.

RESULTS

Moesin's nuclear import is an active, regulated process

Moesin, the actin-binding cytoskeletal protein, is present not just in the cytoplasm, but also in the nucleus as well, where it participates in cellular processes such as transcription and mRNA export (Kristó et al., 2017). Using immunohistochemistry, the nuclear presence of moesin in a steady state is easily observable, but with this method, we do not get any information regarding how the protein is transported into the nucleus. The molecular weight of Drosophila moesin is about 68 kDa which is above the upper limit for passive diffusion through the NPC; therefore, it is a reasonable assumption that moesin translocates into the nucleus by energy dependent, regulated and active transport mechanism.

In order to investigate the dynamics of the nuclear import of moesin, we carried out nuclear FRAP assays on live Drosophila S2R+ cells expressing moesin labeled with GFP on its C-terminus (Moe-GFP). Based on the FRAP experiments carried out on GFP-tagged actin by Dopie et al. (Dopie et al., 2012), first we performed long FRAP assays by monitoring the

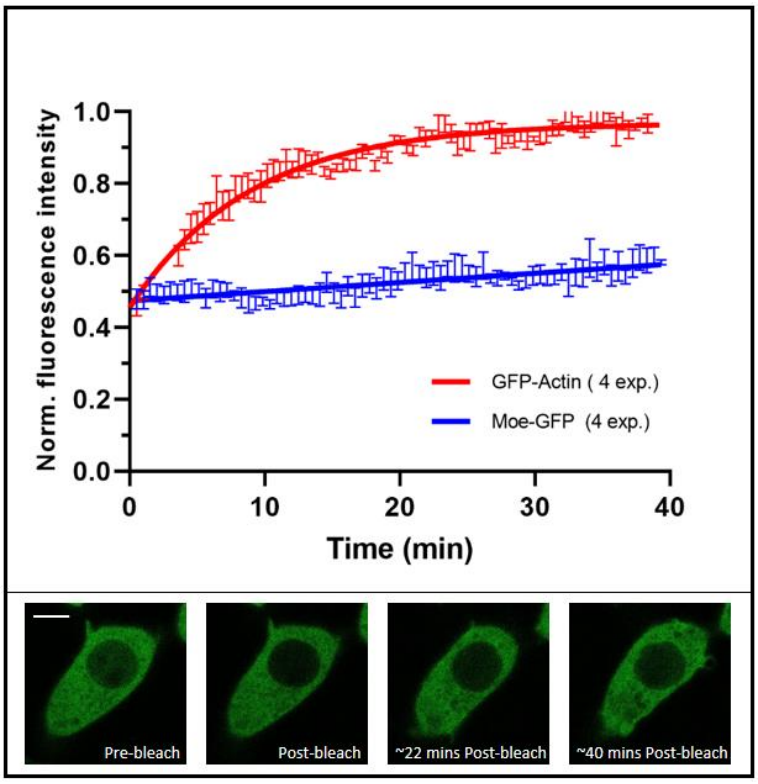

Figure 7. Nuclear import FRAP curves of GFP-tagged actin (red) and moesin (blue). Continuous lines in the graph are curves fitted to the data points, error bars represent standard deviation. Number of replicate experiments are indicated. Images in the bottom show representative phases of a nuclear FRAP assay performed on an S2R+ cell expressing Moe-GFP (green). Scale bar: 5 μm.

recovery of the fluorescent signal from the cytoplasm to the nucleus for 40 minutes after photobleaching the nuclear pool of Moe-GFP. Because in the case of actin, this amount of time was necessary for full recovery after photobleaching, it was plausible that moesin would also need ~40 minutes for a significant or full recovery of nuclear fluorescence. We were surprised, however, because as the resulting FRAP curve shows, the nuclear import dynamics of moesin turned out to be very different from that of actin's (Figure 7). In the case of actin, a fast and dynamic initial recovery of the fluorescent signal can be observed which reflects dynamic nuclear import. In contrast, moesin's nuclear import curve has a very small inclination which is preserved throughout the whole experiment.

This minimal steepness of the curve indicates a low and steady influx of moesin-GFP into the nucleus which is in sharp contrast to the dynamic and fast nuclear import of actin. One might argue that the slight inclination we see with the recovery curve of moesin is not the representation of fluorescent molecules moving into the bleached nucleus, but rather the result of unwanted bleaching of the entire cell created by the consecutive scans. To address this issue, we performed a control experiment called "blind FRAP", in which we follow the distribution of moesin-GFP inside the cell without bleaching (Figure 8). In the case of the unbleached, blind FRAP curve (purple in Figure 8), no recovery of the fluorescent signal can be detected, but a steady and weak fading caused by the scanning with low intensity laser over a longer period of time is observed. Due to this, the curve exhibits a slight declination. This phenomenon is explained by the more pronounced bleaching of Moesin-GFP's nuclear pool which is much smaller than the cytoplasmic pool. However, if we look at the endpoint of the curve, we can see that this unwanted bleaching caused by the scanning itself is negligible, the N/CP fluorescence ratio after 40 minutes of scanning is only about 5% less than at the starting point. In contrast, after a nuclear bleaching event, we can observe a positive, rather than a negative inclination of the curve (blue in Figure 8), and also the steepness of the curve is greater, indicating clearly the nuclear influx of unbleached GFP molecules. Summarizing the results of this first series of experiments, we can say that the nuclear import of moesin is markedly different from one of its main binding partner, actin. While actin shows highly dynamic import, the nuclear transport of moesin is a slow and steady process with nearly constant intensity.

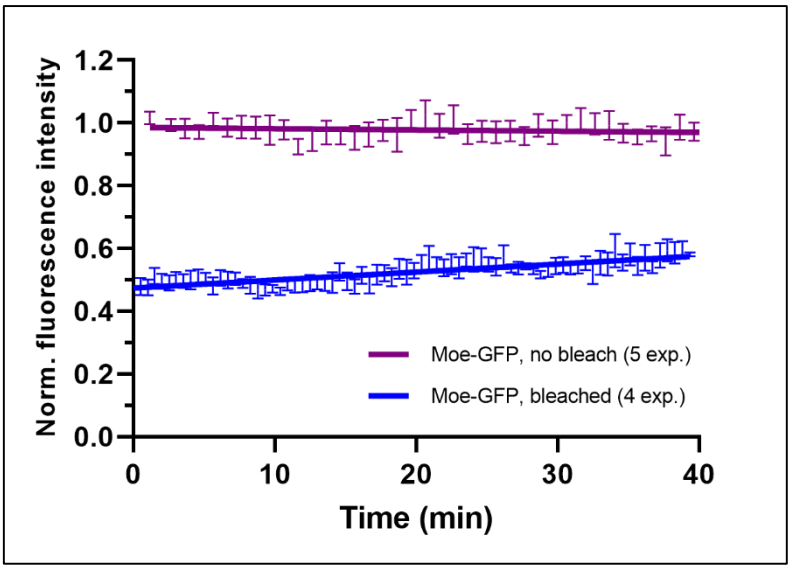

Figure 8. Nuclear import FRAP curves of Moe-GFP, depicting a regular nuclear FRAP assay (blue) and another one, where during the bleaching scans, laser intensity was zero (purple). Continuous lines in the graph are curves fitted to the data points, error bars represent standard deviation. Number of replicate experiments are indicated.

It has been previously shown in our laboratory that upon certain stimuli, such as heat shock or the blocking of mRNA export, moesin accumulates in the nucleus (Kristó et al., 2017). There are multiple possibilities, how increased nuclear amount of moesin can be achieved. One of the explanations is that in response to stimuli, the nuclear import is upregulated and as a result, moesin is transported into the nucleus in much larger quantities than it is transported out of it. It is also feasible that the export of moesin is blocked as a response to the stimulus, resulting in the nuclear accumulation of the protein, even with its weak import dynamics. Once in the nucleus, moesin could also bind strongly to certain nuclear structures which can also cause nuclear accumulation. Finally, it is also possible that the increased amount of moesin in the nucleus is generated by the combination of the aforementioned mechanisms.

To gain insight into the mechanism behind the nuclear accumulation of moesin, we investigated the dynamics of its nuclear import upon blocking mRNA export. For this aim, we treated S2R+ cells expressing moe-GFP with RNA interference (RNAi) targeting the mRNA export factor, Rae1. Nuclear FRAP assays were carried out on these cells using the same parameters of the previous experiments. The resulting FRAP curve, although still significantly below the import dynamics of actin, showed a clearly higher degree of inclination than the FRAP curve observed in untreated cells, suggesting that the rate of import has increased as a consequence of the RNAi treatment (Figure 9). This result tells us that increased nuclear import certainly contributes to the nuclear accumulation of moesin as a response to stress. Furthermore,

we can conclude from the FRAP curve that the nuclear import of moesin is an active, regulated process. Under normal conditions, moesin's nuclear import is downregulated to a low level, but should the need arise for increased presence of the protein in the nucleus, the dynamics of its import can significantly increase.

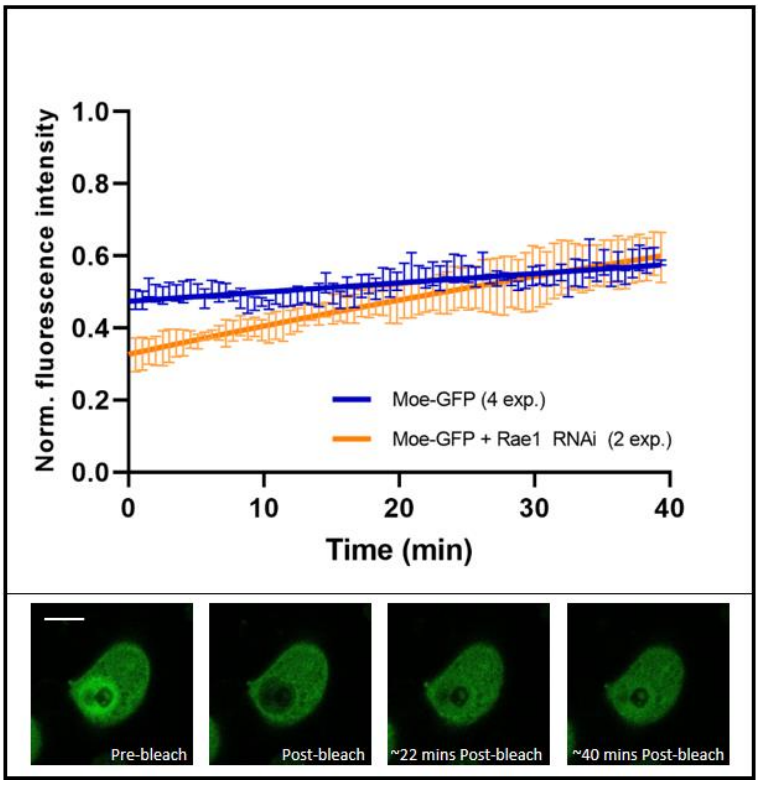

Figure 9. Nuclear import FRAP curves obtained with Moe-GFP under uninduced conditions (blue) and upon induction of nuclear import through *Rae1* RNAi (orange). Continuous lines in the graph are curves fitted to the data points, error bars represent standard deviation.
Microscopic images show an S2R+ cell expressing Moe-GFP (green) and treated with *Rae1* RNAi during a nuclear FRAP assay. Scale bar: 5 μm.

One interesting fact, we can observe in the case of the two FRAP curves is that both of them are linear and do not reach a plateau (Figure 9). A possible explanation for this phenomenon, which we most support, is that in both cases there is some form of inhibition of the nuclear import of moesin. In the case of induced cells, the steepness of the curve is obviously increased, but because it's still linear, the inhibition of moesin's import is likely to be decreased only partially. This model is in good agreement with our previous finding that most of the moesin protein enters the nucleus at the end of cell division, and during interphase the nuclear transport of the protein is not significant (Vilmos et al., 2009; Kristó et al., 2017).

Identification of the NLS of moesin

The results presented above clearly show that moesin does not enter the nucleus by passive diffusion, but rather by a tightly regulated, active process which most likely requires the help of an NLS motif and an importin that recognizes it. To prove this, the NLS of the moesin protein was identified by Ildikó Kristó, Csaba Bajusz and Anikó Szabó in our laboratory. In sum, out of four predicted NLS sites, the RRRK sequence at positions 294-297 (NLS1 or hereinafter referred to as NLS) proved to be responsible for nuclear entry. The motif turned out to be bipartite by including the KR residues 13 amino acids upstream from the NLS sequence ($KR_{X13}RRRK$), at positions 279-280. The activity of the NLS is not controlled by the phosphorylation state of phosphorylatable amino acids in its vicinity (Y292 and T300) as revealed by non-phosphorylatable (Y292A and T300A) and phosphomimetic (Y292D and T300D) amino acid substitutions. To further confirm that the $KR_{X13}RRRK_{297}$ motif is functional, a 27-amino acid fragment containing the NLS was attached to the green fluorescent (GFP) reporter protein. Whereas GFP itself is distributed in both the nucleus and cytoplasm, GFP-MoeNLS highly concentrated in the nucleus, further supporting the idea that the $KR_{X13}RRRK_{297}$ motif is a functional NLS.

The bipartite NLS of moesin shows a high degree of evolutionary conservation

Multiple NLS sites can be predicted in mammalian ERM proteins (Batchelor et al., 2004; Krawetz and Kelly, 2008), out of which the $KR_{X13}RRRK_{297}$ motif was shown to be non-functional, while the sequence corresponding to NLS2 ($RRKQ_{450}$ in *Drosophila melanogaster*) was found necessary for nuclear localization (Batchelor et al., 2004). This is in contrast with our finding however, the nuclear localization of mammalian ERMs was studied only in cultured cells without the induction of nuclear import. On the other hand, vertebrate ERM proteins from human, chicken and clawed frog contain a glutamine in their NLS2 motif (Figure 10A). In addition, the variability of the region corresponding to vertebrate NLS2 is very high in invertebrate ERMs. In fact, the NLS2 motif can only be recognized in starfish and insect proteins, but they also contain glutamine and glutamic acid residues within the sequence, raising serious doubts about the functionality of this motif (Figure 10A).

A

```
HUMAN_EZRIN             ALLEEARRRKEDEVEE
HUMAN_RADIXIN           ALLEEAKKKKEEEATE
HUMAN_MOESIN            SQLEMARQKKESEAVE
MOUSE_EZRIN             ALLEEARRRKEDEVEE
MOUSE_RADIXIN           ALLEEAKKKKEEEATE
MOUSE_MOESIN            SQLEMARKKKESEAVE
BIRD1_MOESIN            TQLELARQKKESEAQE
FROG1_RADIXIN           ALLEEAKKKKEEEASE
FROG1_MOESIN            GQLEFARQKKEEEANE
FISH1_EZRIN             SLLEEAKKRKEEEAQT
FISH1_MOESIN            SLLEDAKKKKEDEALE
FISH2_MOESIN            SLLEDAKKKKEEEAEE
STARFISH_RADIXIN        RELEAQERRKLEECMH
FRUIT FLY_MOESIN        DEVEDARRKQVIAAEA
BEETLE_ERM              EEVENARRKEEELKAQ
MOTH1_ERM               DEVEEARRKQDEAAAL
MOTH2_ERM               EEVEDARRKQDEAAAA
WATER BEAR_ERM          QEVEDAHNRQQAAALA
ROUNDWORM1_ERM          VDAREREVFSMREEVE
ROUNDWORM2_ERM          VDAREREVYTMREEVE
TAPEWORM_ERM            EVEAQKVAMAKKEAEK
HYDRA_RADIXIN           QRLVLEAEAKRKEAAE
SPONGE_ERM              EKKKLEEIAKEKEAAI
CHOANOFLAGELLATE_ERM    QRIRDEATQRDAEVQA
```

B

```
HUMAN_EZRIN             IKPIDKKAPDFVFYAPRLRINKRILQLCMGNHELYMRRRKPDTIEVQQMKAQAREEKHQ
HUMAN_RADIXIN           IKPIDKKAPDFVFYAPRLRINKRILALCMGNHELYMRRRKPDTIEVQQMKAQAREEKHQ
HUMAN_MOESIN            IKPIDKKAPDFVFYAPRLRINKRILALCMGNHELYMRRRKPDTIEVQQMKAQAREEKHQ
MOUSE_EZRIN             IKPIDKKAPDFVFYAPRLRINKRILQLCMGNHELYMRRRKPDTIEVQQMKAQAREEKHQ
MOUSE_RADIXIN           IKPIDKKAPDFVFYAPRLRINKRILALCMGNHELYMRRRKPDTIEVQQMKAQAREEKHQ
MOUSE_MOESIN            IKPIDKKAPDFVFYAPRLRINKRILALCMGNHELYMRRRKPDTIEVQQMKAQAREEKHQ
BIRD1_MOESIN            IKPIDKKAPDFVFYAPRLRINKRILALCMGNHELYMRRRKPDTIEVQQMKAQAREEKHQ
FROG1_RADIXIN           IKPIDKKAPDFVFYAPRLRINKRILALCMGNHELYMRRRKPDTIEVQQMKAQAREEKHQ
FROG1_MOESIN            IKPIDKKAPDFVFYAPRLRINKRILALCMGNHELYMRRRKPDTIEVQQMKAQAREEKHQ
FISH1_EZRIN             IKPIDKKAPDFVFYAPRLRINKRILQLCMGNHELYMRRRKPDTIEVQQMKAQAREEKQQ
FISH1_MOESIN            IKPIDKKAPDFVFYAQRLRINKRILALCMGNHELYMRRRKPDTIEVQQMKAQAKEEKNH
FISH2_MOESIN            IKPIDKKAPDFVFYAPRLRINKRILALCMGNHELYMRRRKPDTIEVQQMKAQAREDKNH
STARFISH_RADIXIN        IKPIDKKAPDFVFFAERLRINKRILALCMGNHELYMRRRKPDTIEVQQMKAQAREEKSS
FRUIT FLY_MOESIN        IKPIDKKAPDFMFFAPRVRINKRILALCMGNHELYMRRRKPDTIDVQQMKAQAREEKNA
BEETLE_ERM              IKPIDKKAPDFVFFAPRVRINKRILSLCMGNHELYMRRRKPDTIDVQQMKAQAREEKLA
MOTH1_ERM               IKPIDKKAPDFVFFAPRVRVNKRILALCMGNHELYMRRRKPDTIDVQQMKAQAREEKLA
MOTH2_ERM               IKPIDKKAPDFVFFAPRVRVNKRILALCMGNHELYMRRRKPDTIDVQQMKAQAREEKLA
WATER BEAR_ERM          IKPIDKKAPDFVFFASRLRINKRILALCMGNHELYMRRRKPDTIEVQQMKAQAREEKVA
ROUNDWORM1_ERM          IKPIDKKAHDFVFYAPRLRINKRILALCMGNHELYMRRRKPDTIEVQQMKQQAREDRAL
ROUNDWORM2_ERM          IKPIDKKAHDFVFYAPRLRINKRILALCMGNHELYMRRRKPDTIEVQQMKQQAREERAL
TAPEWORM_ERM            IKPADKSAKEFFFLVEKSKINKRILALCTGNHELYMRRRKSDSIEVQQMKIQAKEEREL
HYDRA_RADIXIN           IKPIDRKAPDFLFYVPRLRINKRILSLCMGNHELYMRRRKPDTIEVQQMKAQAREEKQG
SPONGE_ERM              IKPIDKKAPDFVFNAPRLRINKRILALCMGNHELYLRRRKPDTIEVQQMKAQAREEKIS
CHOANOFLAGELLATE_ERM    IKPIDKKAPDFIFLATRLRINKRILALCMGNHELYMRRRRPDSIEVQQMKAQAREEKAI
                        *** **.* :*.* . : ::***** ** ******:***: *:*:***** **:*::
```

Figure 10. Clustal Omega multiple sequence alignment of the region around the potential NLS sequences of various ERM proteins found across the kingdom Metazoa (Animalia). The NLS motifs are highlighted in yellow. **A)** The conservation of $RRKQ_{450}$ (NLS2) sequence. The horizontal line separates vertebrate and invertebrate species. Non-conserved residues are highlighted in turquoise. **B)** The conservation of the $KR_{X13}RRRK_{297}$ NLS motif. The horizontal line separates vertebrate and invertebrate species. Phosphorylatable residues are highlighted in green. Asterisks (*) indicate positions which have a single, fully conserved residue, colon (:) indicates conservation between groups of strongly similar properties, subscript period (.) indicates conservation between groups of weakly similar properties, no mark indicates no conservation. Species names and protein accession numbers can be found in Table 1. in the Appendices section.

To see, whether the NLS identified by us in Drosophila moesin can also be found in the ERM proteins of other species, we performed multiple sequence alignments of 24 ERM proteins found in 18 different species. The analysis revealed that the bipartite NLS identified in moesin

is evolutionary highly conserved. This conservation not only applies to the two parts of the NLS motif itself, but also to the distance between them (Figure 10B). The high degree of evolutionary conservation of the NLS and the immediate region surrounding it indicates that the residues found here are indeed important for the proper functioning of ERM proteins.

Investigating the possible regulation of the NLS through phosphorylation

In the vicinity of the bipartite NLS of moesin there are two phosphorylatable amino acids, a tyrosine (Y292) and a threonine residue (T300). However, my colleagues have previously found that the substitution of them with phosphomimetic aspartic acid (Y292D and T300D) has no effect on the nuclear import of moesin, we decided to confirm this result by mutating the residues to the other phosphomimetic residue, glutamic acid.

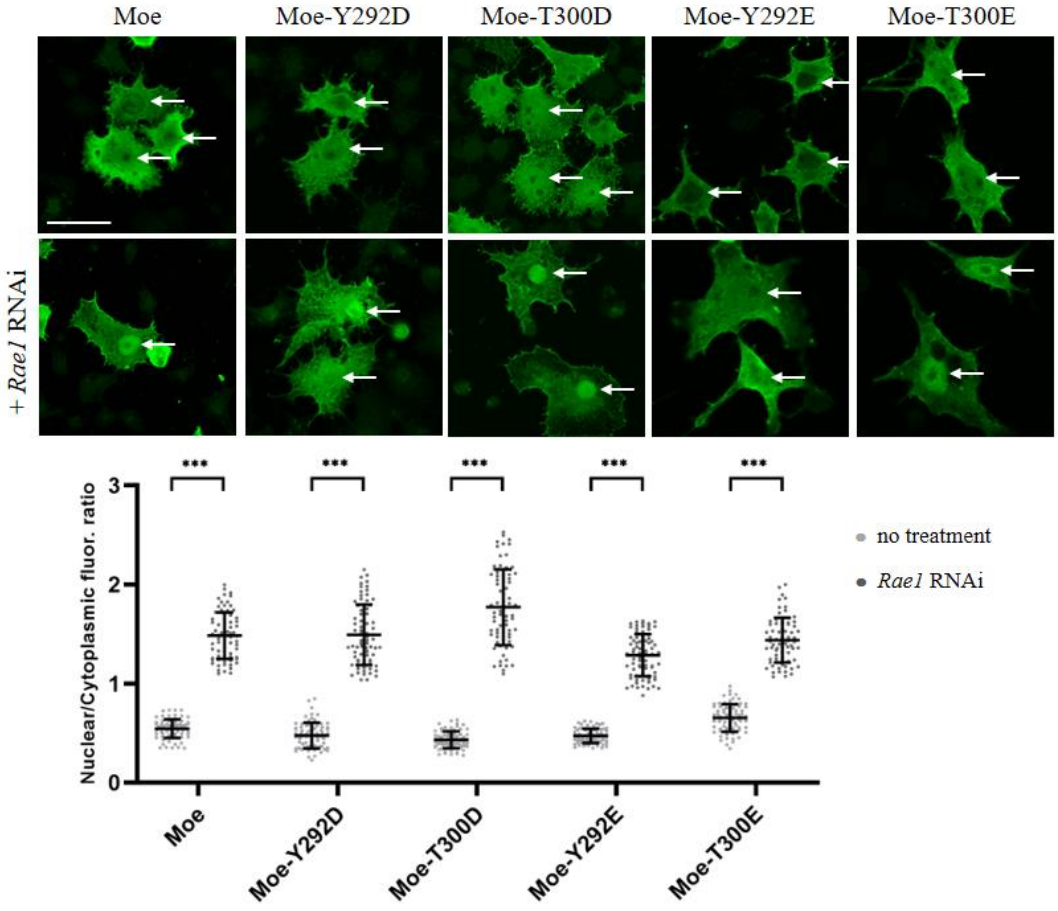

Figure 11. Subcellular localization of the phosphomimetic MoeY292 and T300 mutants. White arrows mark the nuclei. Scale bar: 10 μm.
Graph shows the quantification of immunostainings. Nuclear/cytoplasmic pixel intensity ratios were calculated. Data represent mean rates, error bars represent standard deviation. *p*-values: ***: $p<0.001$.

The nuclear import of MoeY292E and MoeT300E proteins was evaluated by transfecting Drosophila S2R+ cells with plasmids encoding the GFP-tagged versions of the mutant proteins, and nuclear import was induced by *Rae1* RNAi treatment. The experiment revealed that all of the phosphomimetic variants of moesin were able to accumulate in the nucleus upon import induction (Figure 11), providing additional evidence that the phosphorylation of these amino acids in the vicinity of the NLS are not regulating the nuclear localization of moesin.

Closed conformation is preferred in nuclear import

As discussed in the introduction, ERM proteins exist in open (active) or closed (inactive) conformational states in the cell. To obtain an open, protein-binding form, moesin must, among other things, be phosphorylated at a threonine residue near its C-terminus (T559). In order to investigate which conformational form of the protein is import-competent, we generated the point mutants MoeT559D and MoeT559A, which were already described in the literature previously (Polosello et al., 2002). In MoeT559D, the threonine is mutated to the phosphomimetic aspartic acid; therefore, this mutant is in an open, constitutively active state. In contrast, the MoeT559A protein carries a non-phosphorylatable alanine residue in place of T559, therefore the protein cannot get into a stably active state and thus, it is unable to bind its partners.

As a preliminary experiment, we first tested whether there is a true difference between the activity of the two mutant proteins. For this aim, we expressed the GFP-tagged MoeT559 mutant proteins in S2R+ cells, and monitored their subcellular localization and binding through cortical FRAP assay. Moesin is capable of binding F-actin and various proteins of the plasma membrane in its open, active conformation. Because of this, we expected strong interactions between MoeT559D and the cortical F-actin network and the membrane proteins which causes a prominent localization at the cell cortex. In contrast, no cortical localization was expected from the inactive mutant form, MoeT559A which is not capable of protein binding. When we looked at the transfected cells, the difference between the localization of the two mutant forms was striking. MoeT559D was primarily present at the plasma membrane, while MoeT559A exhibited a diffuse, homogeneous distribution in the cytoplasm (Figure 12, lower part). The cortical FRAP assays further confirmed the functional difference between the two mutant forms (Figure 12, upper part). Comparing the FRAP curves obtained with the two mutant proteins, key differences can be observed. In contrast to the FRAP curve of MoeT559D, the curve of MoeT559A exhibits a smaller bleaching depth (the amount of bleached molecules compared to

pre-bleach state), even though the bleaching parameters were the same in the two experiments. This indicates that the GFP fluorophores in the ROI (region of interest; the bleached area) exchanged even during the bleaching event which phenomenon can be explained by the high mobility of the protein. Secondly, the plateau of the MoeT559A curve (the state, when maximal recovery of mobile fluorophores is achieved in the ROI) is reached much faster, than in the case of MoeT559D. This also tells us that there is a fast turnover of unbound molecules of MoeT559A in the cortex area. Lastly, normalized fluorescence intensity in the ROI after reaching the plateau of recovery is about 90% in the case of MoeT559A, compared to about 78% with MoeT559D which indicates that a larger percentage of bleached fluorescent

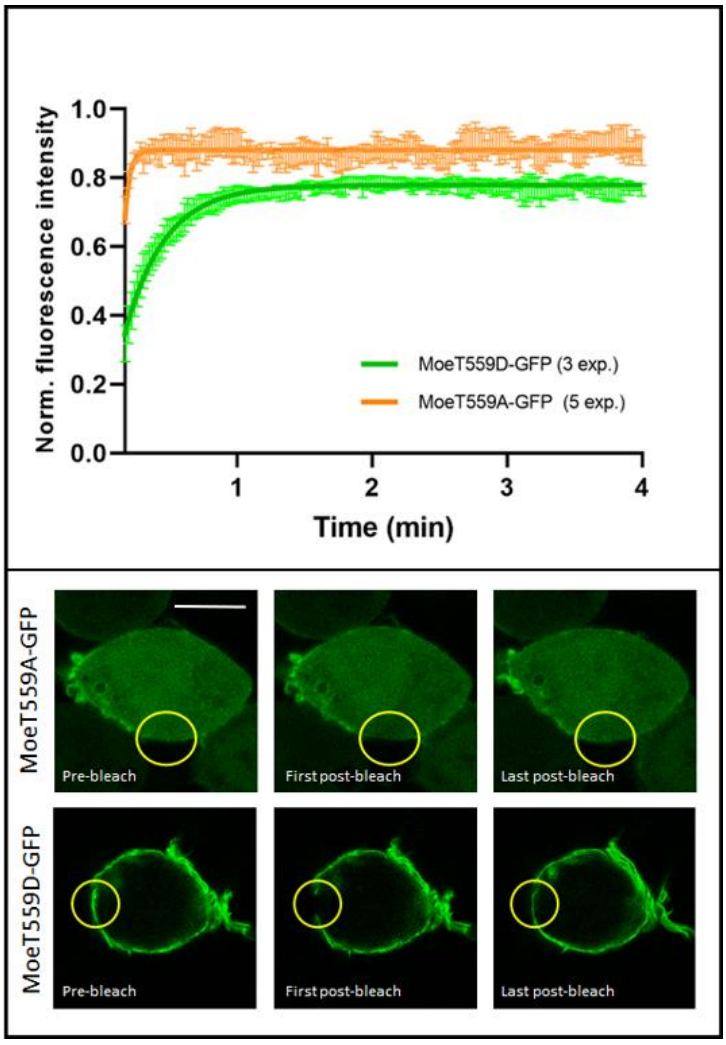

Figure 12. FRAP assays performed at the cell cortex with GFP-tagged MoeT559A (brown) and MoeT559D (green) proteins. Continuous lines in the graph are curves fitted to the data points, error bars represent standard deviation. Number of replicate experiments are indicated.
Pictures in the lower part show representative cells from the experiments. Yellow circles mark the ROIs (sites of bleaches) at the cortex. Scale bar: 5 μm.

molecules could be exchanged for unbleached ones in the ROI during the recovery phase of the experiment. This higher ratio of exchange can be explained by the lack of strong interactions between the inactive moesin mutant and other potential binding partners in the ROI. All these differences of the FRAP curves support the notion that the MoeT559D form localizes mostly to the cell cortex, where it forms stable intermolecular interactions with F-actin and proteins of the plasma membrane. However, MoeT559A does not show pronounced cortical localization which obviously suggests that it cannot form stable molecular connections there.

As the results of the cortical FRAP experiments supported the functional difference between the two MoeT559 mutants, we carried out the nuclear import FRAP assays with them. The resulting FRAP curves revealed that the nuclear import dynamics of the two mutant proteins are very similar (Figure 13). Neither of them takes on a sharp initial recovery after photobleaching, as seen for example in the case of GFP-actin which would indicate a fast, dynamic nuclear import. Instead, both mutants exhibit a recovery curve similar to wild-type moesin, indicating slow and steady influx into the nucleus. This suggests that both mutant forms are able to enter the nucleus similarly to the wild-type protein. This brings us to the conclusion that moesin's nuclear import is not regulated through its conformation.

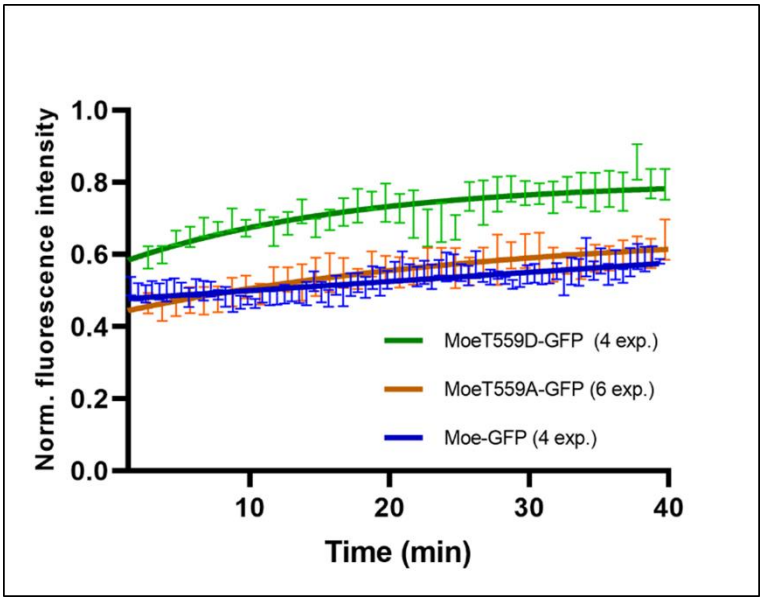

Figure 13. Nuclear import FRAP curves of GFP-tagged MoeT559A (inactive mutant, brown curve) and MoeT559D (active mutant, green curve) proteins compared to wild-type, GFP-tagged moesin (blue curve). Continuous lines in the graph are curves fitted to the data points, error bars represent standard deviation. Number of replicate experiments are indicated.

To further investigate the nuclear import capability of the different protein conformations, transfected cells expressing the active and inactive protein forms were immunostained (Figure 14). The import was induced by *Rae1* RNAi and, like in the FRAP experiments, it was found that both conformations of moesin could enter and accumulate in the nucleus. At the same time, it is important to note that the quantification of the immunostainings shows that the active, TD form is apparently present in the nucleus in much smaller amounts after import induction, than the inactive and wild-type conformations. This means that although the dynamics of entry into the nucleus do not differ in the case of the mutant forms, the inactive, closed-conformation form is still able to enter the nucleus in larger quantities. The observation can be explained by the molecular interactions which retain the active form of moesin at the cell membrane.

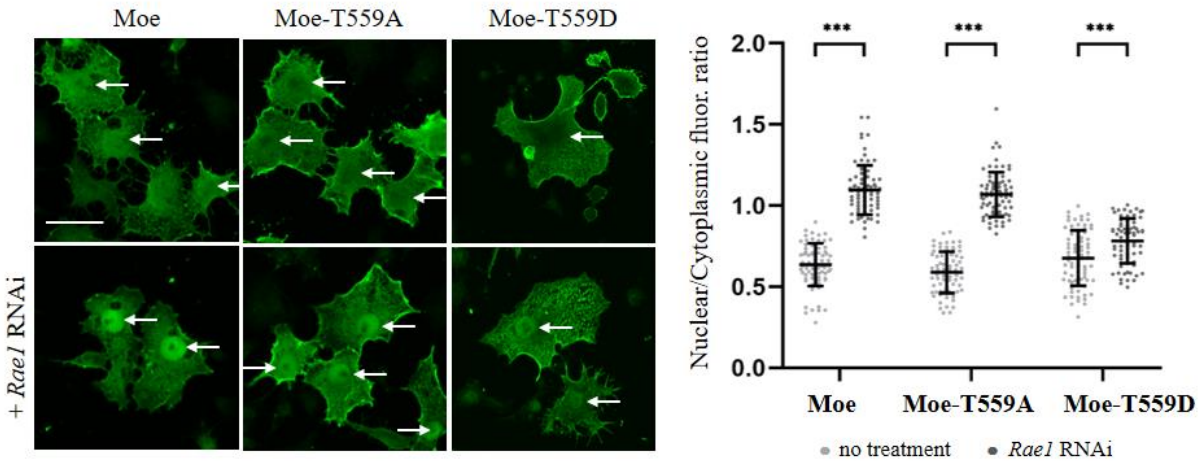

Figure 14. Nuclear accumulation of MoeT559 mutants (green) upon induction of import (*Rae1* RNAi). White arrows mark the nuclei. Scale bar: 10 μm.
Graph shows the quantification of immunostainings. Nuclear/cytoplasmic pixel intensity ratios were calculated. Data represent mean rates, error bars represent standard deviation. *p*-values: ***: $p<0.001$.

To explore the idea that the closed conformation is preferred for nuclear entry, we examined how the inhibition of the Slik kinase, which phosphorylates T559 in Drosophila moesin and thereby stabilizes its active state (Hipfner et al., 2004), affects the import (Figure 15). Simple main effects statistical analysis showed that *Slik* RNAi treatment alone had a significant effect on N/CP ratio ($p = 5.8\text{x}10^{-15}$), it increased the amount of moesin in the nucleus even without the induction of import. There was a statistically significant interaction also between the effects of *Rae1* and *Slik* RNAi treatments ($p = 1.2\text{x}10^{-10}$) (Figure 15). These results provide more evidence that the non-phosphorylated form of moesin is favored in nuclear import.

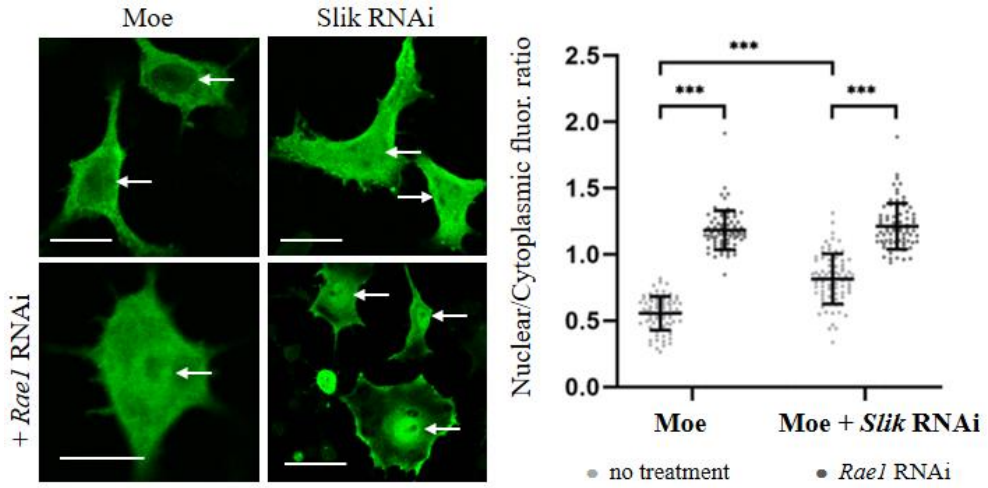

Figure 15. The effects of *Slik* and *Rae1* RNAi treatments on the subcellular localization of moesin. White arrows mark the nuclei. Scale bars: 10 μm.
Graph shows the quantification of immunostainings. Nuclear/cytoplasmic pixel intensity ratios were calculated. Data represent mean rates, error bars represent standard deviation. *p*-values: ***: $p<0.001$.

Investigation of F-actin binding as a possible regulator of the nuclear import of moesin

The main binding partner of moesin, actin is one of the most abundant proteins in eukaryotic cells. In the cell actin can be present in two forms, as monomeric G-actin or filamentous F-actin. On the C-terminus of moesin there is a dedicated F-actin binding site which is essential for moesin to be able to perform its main role in the cytoplasm, that is, the anchoring of the actin cytoskeleton to the plasma membrane. There are known examples in the literature, in which the balance between the G- and F-actin pools is responsible for the subcellular localization of a protein that is capable of actin binding. A prime example of this phenomenon is that of the SRF (**S**erum **R**esponse **F**actor) coactivator, MAL (**M**egakaryocytic **A**cute **L**eukemia, also known as MKL1 (**M**ega**k**aryoblastic **L**eukemia **1**) or MRTFA (**M**yocardin **R**elated **T**ranscription **F**actor **A**) in human) (Miralles et al., 2003). Without serum induction, MAL localizes to the cytoplasm. This is facilitated by it binding to G-actin which prevents the nuclear translocation of MAL. Upon serum induction, the balance between G- and F-actin is shifted towards the filamentous form, as a result of which the amount of free G-actin decreases in the cytoplasm. This also means that the actin monomers that bind MAL will release it in order to get incorporated into actin filaments. At this point, the now unbound MAL becomes nuclear transport-competent and gets imported into the nucleus, where it takes part in the transcriptional response to serum stimulation.

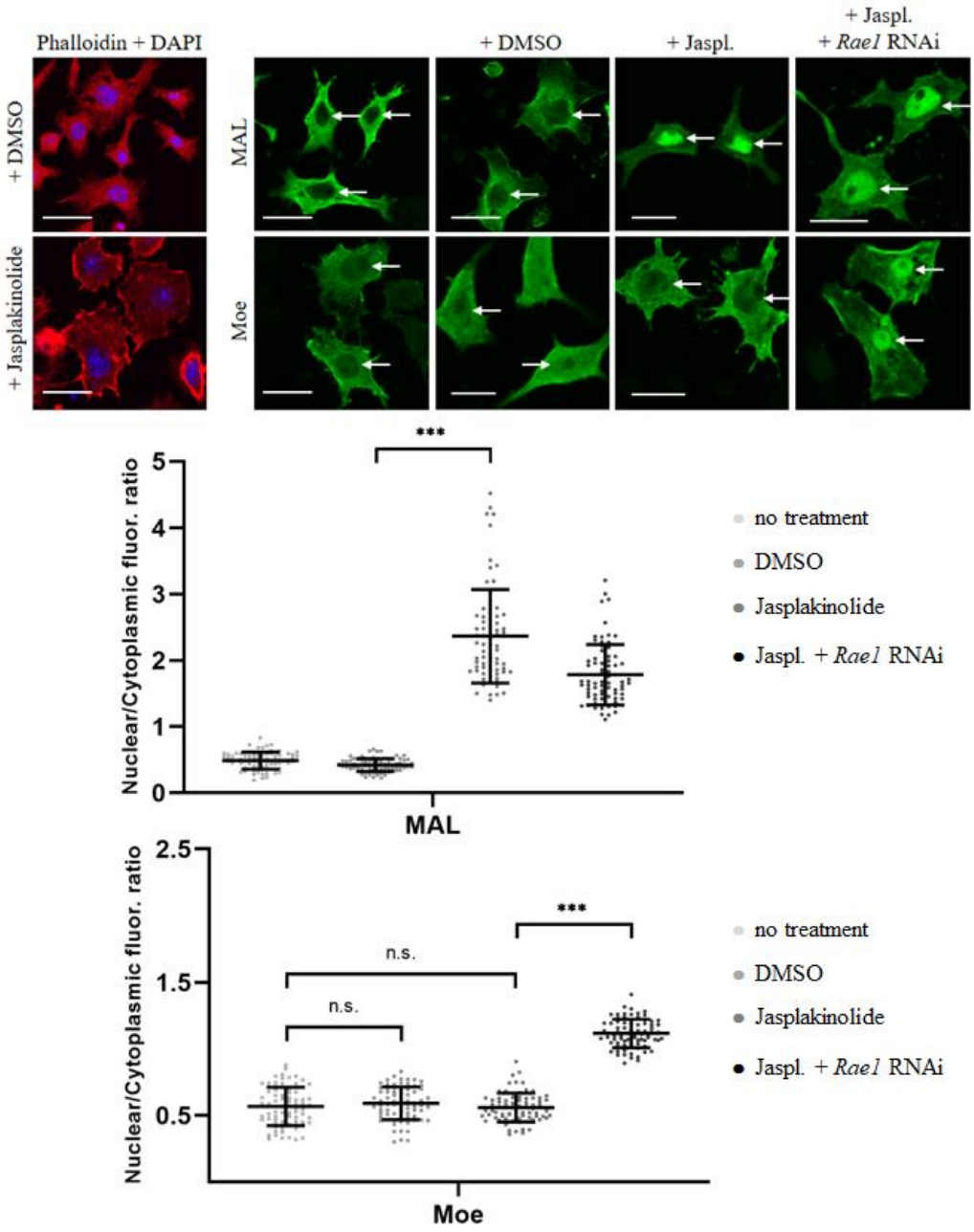

Figure 16. Effect of Jasplakinolide treatment on the subcellular localization of GFP-tagged MAL (green, upper row) and moesin (green, lower row) proteins. Phalloidin staining (red, left side) was used to establish the effectiveness of Jasplakinolide treatment. White arrows mark the nuclei. Scale bars: 10 μm.
Graphs show the quantification of immunostainings. Nuclear/cytoplasmic pixel intensity ratios were calculated. Data represent mean rates, error bars represent standard deviation. *p*-values: ***: $p<0.001$, n.s.: $p>0.05$.

In order to investigate, whether actin has a role in the regulation of the subcellular localization of moesin in a manner similar to that of MAL, we treated Drosophila S2R+ cells expressing Moe-GFP with Jasplakinolide, a cytoskeletal drug that promotes actin

polymerization. With this treatment we reduced the pool of free G-actin and at the same time increased the amount of F-actin. To make sure that the drug treatment was effective, the microfilament network was visualized with Phalloidin staining, and as a control condition, we also looked at the subcellular distribution of the MAL protein (Figure 16). *Rae1* RNAi was applied to induce the nuclear import of moesin. The status of the actin cytoskeleton and the change in the subcellular distribution of MAL demonstrated that the Jasplakinolide treatment was effective (Figure 16). However, we found that increasing the amount of F-actin and simultaneously reducing the pool of available G-actin does not result in any noticeable change in the nuclear import of moesin, the protein can still accumulate in the nucleus upon import induction (Figure 16). This indicates that monomeric actin is neither hindering nor is necessary for the nuclear translocation of moesin.

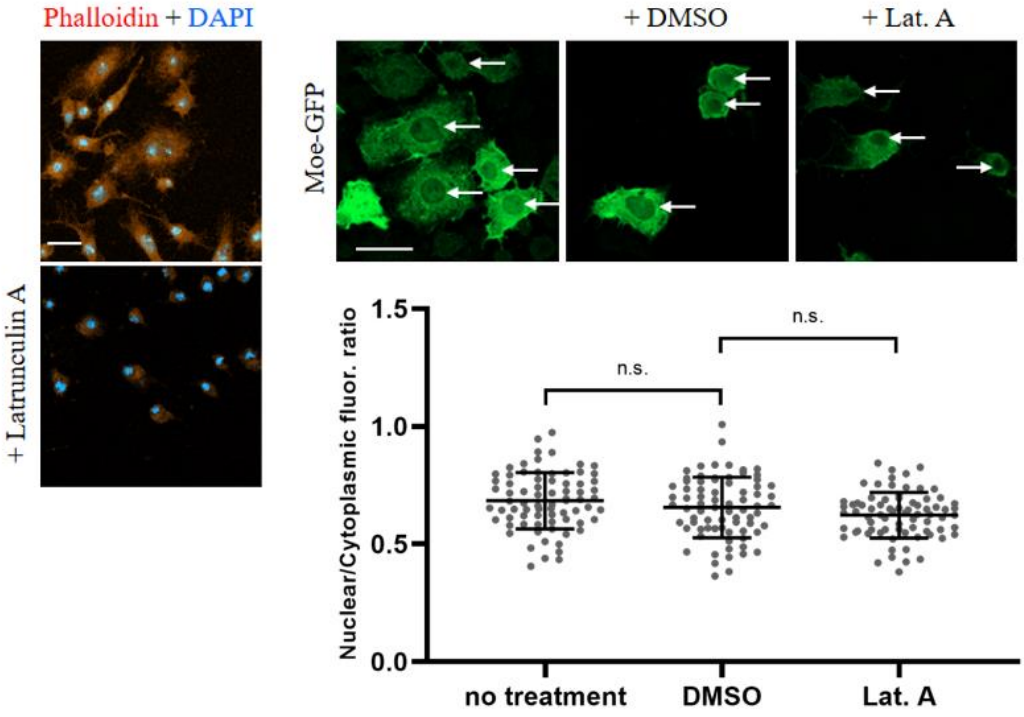

Figure 17. Effect of Latrunculin A treatment on the subcellular localization of GFP-tagged moesin (green). Phalloidin staining (red, left side) was used to control the effectiveness of Latrunculin A treatment. The experiment was performed by Ildikó Kristó. White arrows mark the nuclei. Scale bars: 10 μm.
Graph shows the quantification of immunostainings. Nuclear/cytoplasmic pixel intensity ratios were calculated. Data represent mean rates, error bars represent standard deviation. *p*-values: n.s.: $p>0.05$.

After decreasing G-actin levels with Jasplakinolide, we approached the problem also from the other direction. In this experiment, which was carried out by my colleague Ildikó Kristó,

the amount of free monomeric actin was increased with the help of a cytoskeletal drug. The sponge toxin Latrunculin A (Lat. A) prevents actin polymerization by binding to G-actin near the nucleotide binding cleft, and it also enhances actin depolymerization, resulting in the increase of the amount of free G-actin in the cell. According to the control staining with Phalloidin, Lat. A effectively disrupted the F-actin network (Figure 17). Upon inspection of the localization of moesin in treated cells, we concluded that the depolymerization of the actin network had no effect on the nuclear import of the protein (Figure 17) which means also that it is not F-actin binding that inhibits the nuclear import of activated moesin.

Identification of a cytoplasmic retention signal in moesin

Based on the results presented so far, it is clear that moesin has a functional bipartite NLS which upon certain stimuli is able to enhance the nuclear import of the protein. But the FRAP results revealed that even in the case of increased import, the dynamics of nuclear entry is still low. Our attempt to show whether the nuclear import of moesin is regulated by phosphorylation (MoeY292 and MoeT300 mutants), F-actin binding or conformation (MoeT559 mutants) did not clarify the mechanism behind moderate import. The most plausible explanation for this would be some form of cytoplasmic retention since binding to a cytoplasmic partner would explain the slow, steady influx of moesin into the nucleus. As discussed in the introduction section, several proteins are known whose subcellular localization is regulated by some form of cytoplasmic retention mechanism. It was therefore a reasonable assumption that in the case of moesin, something similar might be happening.

The FERM domain containing protein, merlin (also known as neurofibromin 2 (NF2) or schwannomin) is a close relative of ERM proteins. Merlin shares multiple similarities with the ERM proteins, for example it also has an N-terminal FERM and a C-terminal F-actin binding domain. The activity of merlin is also conformationally regulated in a manner similar to the ERMs. In its inactive state, the N-terminal FERM and the C-terminal domains of merlin self-associate, creating a stable, closed conformation. Located in exon 2 of merlin which corresponds to part of its FERM domain, there is a sequence that was described as responsible for the cytoplasmic retention of the protein. Upon deletion of this exon, the mutant protein is able to enter the nucleus in a considerable amount. However, because merlin also has a functional and highly active NES sequence, this newly acquired nuclear entry capability could only be observed when its nuclear export was simultaneously blocked by the CRM1 export pathway inhibitor Leptomycin B (Kressel and Schmucker, 2002).

Upon comparing the region of human merlin's exon 2 identified as responsible for cytoplasmic retention with the corresponding region of Drosophila merlin and of Drosophila moesin, a high degree of similarity was found with multiple amino acids being identical (Figure 18). Therefore, we decided to test whether moesin possesses a retention motif in this region (hereafter referred to as: Cytoplasmic Retention Signal or CRS for short) that could be responsible for its retention in the cytoplasm. To this aim, we generated the deletion mutant called MoeΔCRS, in which 10 amino acids ($FDQVVKTIGL_{40}$) were deleted from the middle of the potential, 25 amino acids long CRS sequence of moesin.

```
HUMAN_MERLIN          FTVRIVTMDAEMEFNCEMKWKGKDLFDLVCRTLGLRETWFFGLQYTI-KDTVAWLKMDKK
FRUIT FLY_MERLIN      LSVRVSTFDSELEFKLEPRASGQDLFDLVCRTIGLRESWYFGLQYVDTRSNVSWLKMEKR
FRUIT FLY_MOESIN      LNVRVTTMDAELEFAIQSTTTGKQLFDQVVKTIGLREVWFFGLQYTDSKGDSTWIKLYKK
                      :.**: *:*:*:**  :   .*::*** * :*:**** *:*****.  :.  :*:*: *:
```

Figure 18. Clustal Omega alignment of the protein sequences around the CRS in human merlin, Drosophila merlin and Drosophila moesin proteins. Conserved residues of the CRS identified in human merlin and the corresponding sequences in the other two proteins (25 amino acids) are highlighted in yellow. Asterisks (*) indicate positions which have a single, fully conserved residue, colon (:) indicates conservation between groups of strongly similar properties, subscript period (.) indicates conservation between groups of weakly similar properties, no mark indicates no conservation.

We found that the subcellular localization of the GFP-tagged version of the MoeΔCRS mutant is remarkably different from that of the wild-type protein. Interestingly, MoeΔCRS localizes primarily to the plasma membrane and also to filopodia (Figure 19, lower part, first picture). However, the amount of the mutant protein in the nucleus is not markedly different from that of the wild type.

In order to confirm a possible role the CRS might play in the regulation of the nuclear import of moesin, we carried out nuclear import FRAP assays on S2R+ cells expressing GFP-tagged MoeΔCRS. We found that the dynamics of import changed dramatically compared to either the wild type, or any other mutant form we have created and tested so far (Figure 19). When looking at the FRAP curve of the MoeΔCRS mutant, we can see that right after the bleaching scans the recovery of the signal begins instantaneously and rapidly, indicating a significant and dynamic influx of the unbleached fluorescent protein into the nucleus. This initial sharp rise gets to the plateau phase just a few minutes (~4 minutes) after the bleaching event. In contrast to this, in the case of the wild-type protein not even 40 minutes were enough for the signal to reach full recovery after bleaching, even when nuclear import was induced by *Rae1* RNAi. The result of the nuclear import FRAP experiment suggests that moesin indeed

has a functional cytoplasmic retention sequence that plays a key role in the regulation of its subcellular localization.

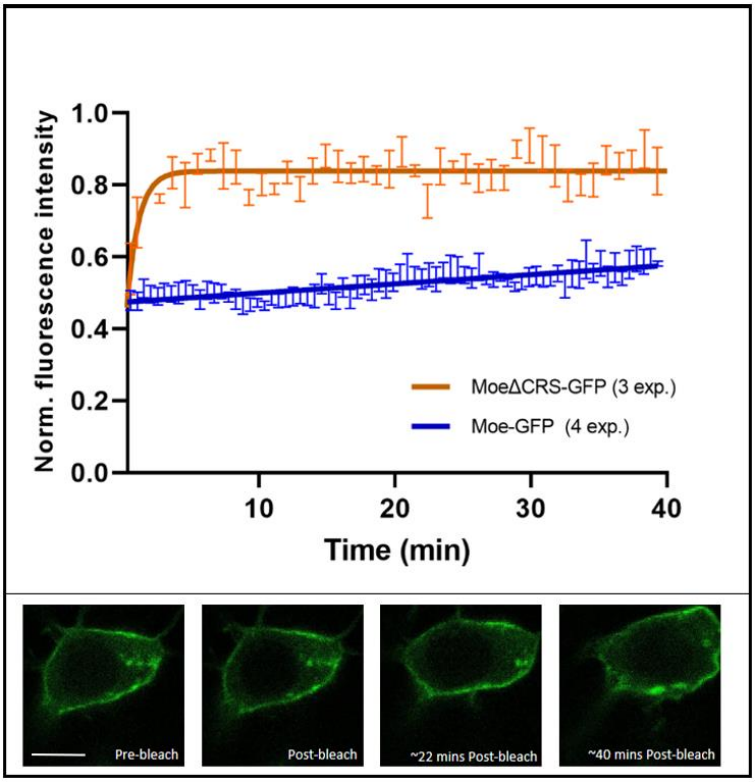

Figure 19. Nuclear import FRAP curve obtained with the MoeΔCRS mutant protein (brown) compared to wild-type, GFP-tagged moesin (blue). Continuous lines in the graph are curves fitted to the data points, error bars represent standard deviation. Number of replicate experiments are indicated in the graph.
Microscopy images show an S2R+ cell expressing MoeΔCRS-GFP (green) during a nuclear FRAP assay. Scale bar: 5 μm.

To further study and characterize the functionality of this newly identified CRS sequence, we designed an experimental system in which we tagged an indifferent protein, the GFP, with different parts of the moesin CRS and its vicinity. The GFP protein has a molecular weight of 27 kDa, which is below the upper limit (~60 kDa) of passive diffusion, therefore it is found in ample amounts both in the nucleus and in the cytoplasm. It should also be noted here that when GFP is expressed in cells, the fluorescent signal is often stronger in the nucleus than in the cytoplasm (see for example Salichs et al., 2009; Schwarzerova et al., 2019). The basic idea of the experiment is that if any of the CRS tags fused to GFP can cause the retention of the GFP in the cytoplasm, we should see a decrease in the nuclear levels of the given fusion protein.

Five such GFP and CRS fusion constructs were designed and created. In the **GFP-CoreCRS** protein the GFP was fused with 12 amino acids that contains 8 of the 10 residues deleted in the MoeΔCRS mutant, and which form an alpha-helix in the 3D structure of moesin.

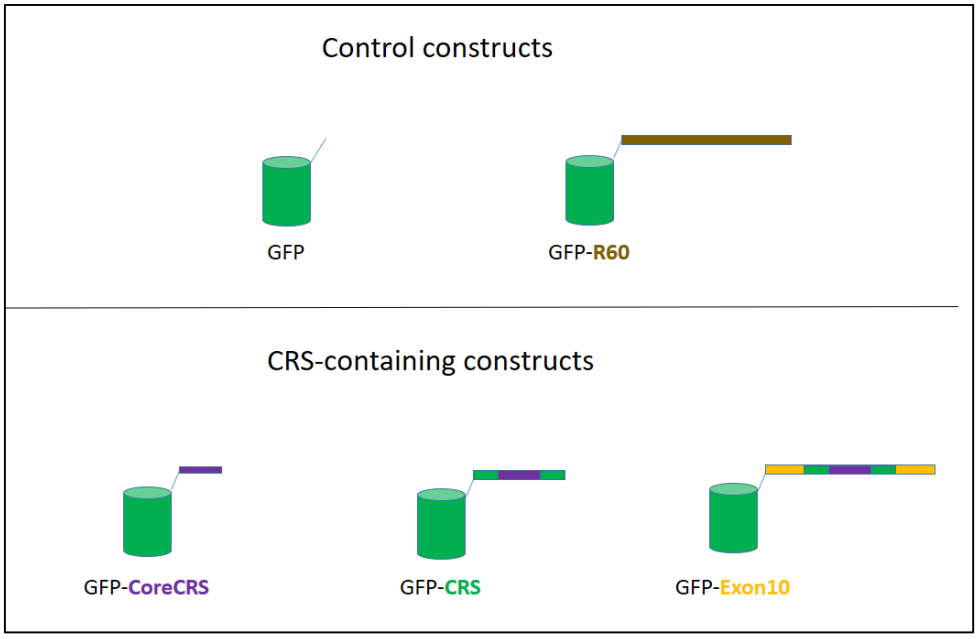

Figure 20. Summary of the protein constructs used in the "GFP-CRS tag" experiment. Green „barrels" represent GFP. Thick, horizontal lines of various colors represent the different tags.

The **GFP-CRS** protein contains a 25 amino acids-long sequence of Drosophila moesin that corresponds to the CRS identified by Kressel and Schmucker in mouse merlin. In the case of **GFP-Exon10**, 60 amino acids encoded by exon 10 of moesin, which also contains the CRS, were attached to GFP. As controls for the experiment, we used two additional proteins. One of them was **GFP** itself, without any tag. In the other control protein, named GFP-R60, a protein with a random sequence of 60 amino acids, the size of which is the same as the protein encoded by exon 10, was attached to GFP (Figure 20).

When investigating the distribution of the CRS-tagged fusion proteins inside the transfected cells, we could observe that the controls, GFP and GFP-R60, showed similar localization patterns. In these cases, fluorescence can be detected both in the nucleus and the cytoplasm, with the nuclear signal being stronger (Figure 21). This is in concert with the known intracellular distribution of GFP. The fact that GFP-R60 shows the same distribution as GFP itself indicates that the size of the tag fused to GFP does not influence its localization. This result is consistent with the literature since the calculated molecular mass of the GFP-R60

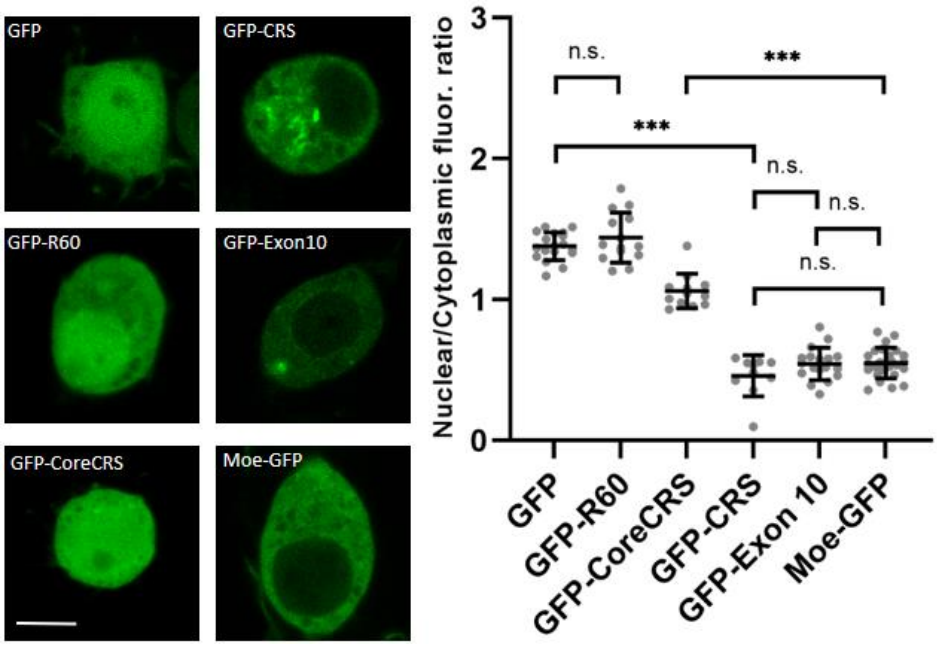

Figure 21. Intracellular distribution of GFP tagged with CRS tags of various sizes (green) in live S2R+ cells.
Graph shows nuclear/cytoplasmic pixel intensity ratios. Data represent mean rates, error bars represent standard deviation. *p*-values: ***: $p<0.001$, n.s.: $p>0.05$.

protein (~35 kDa) is well below the weight limit of passive diffusion. The intracellular distribution of the CRS-tagged versions of GFP revealed that the 10 amino acids, which compose the "CoreCRS" sequence, are not enough to retain the protein in the cytoplasm, hence it is present in the nucleus in significant amount. However, both of the remaining tags, "CRS" and "Exon10" were able to prevent nuclear entry of most of the GFP. Their subcellular distribution was quite similar to that of GFP-tagged wild-type moesin, although the molecular weight and size of both constructs should still allow for passive diffusion through the NPC. These results indicate that the 25 amino acids long CRS sequence is enough to prevent nuclear entry of a protein and is most likely also responsible for this phenomenon in the case of full-length, wild-type moesin (Figure 21).

To further confirm our finding that the CRS sequence of moesin in indeed functional, we analyzed the nuclear import dynamics of some of the constructs used in the previous experiment by nuclear FRAP assay. Since GFP can get through the NPC unrestrictedly by passive diffusion, we can see that right after photobleaching the nucleus, the recovery begins immediately, and maximum recovery, which is about 90%, is reached in less than two minutes. This demonstrates a fast and dynamic nuclear influx of GFP (Figure 22). When examining the dynamics of the

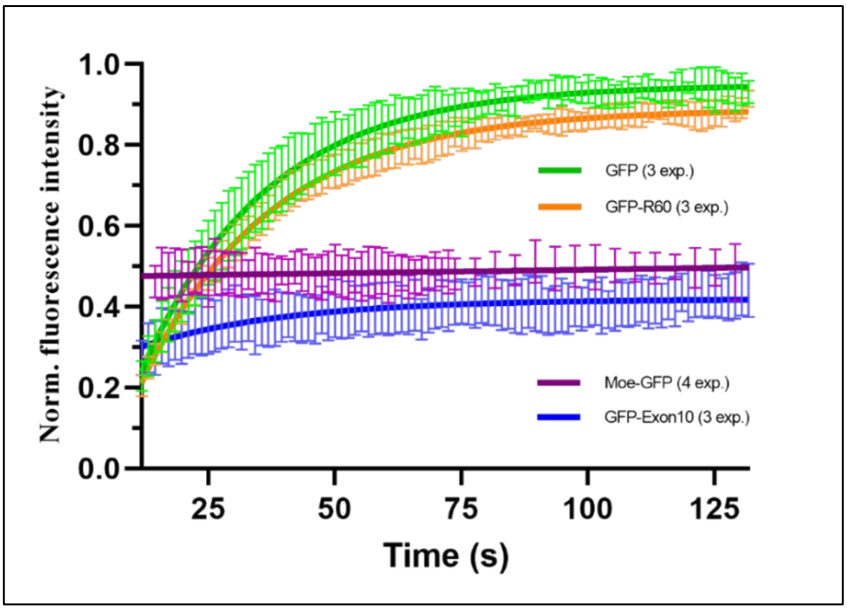

Figure 22. Nuclear import FRAP curves of GFP-CRS constructs. GFP-R60 (brown), used to control tag size, translocates into the nucleus just as dynamically as GFP itself (green). The nuclear import of the CRS-tagged GFP construct (GFP-Exon10 in purple) is blocked in the same way as Moe-GFP (blue). Continuous lines in the graph are curves fitted to the data points, error bars represent standard deviation. Number of replicate experiments are indicated.

nuclear translocation of GFP-R60, we can observe a very similar curve, indicating that the size of the tag fused to GFP does not influence the dynamics of nuclear translocation. In contrast, GFP-Exon10, which has the same size as GFP-R60 (~35 kDa) but contains the CRS sequence, shows a different curve, suggesting weak nuclear import activity. The FRAP curve in this case is extremely similar to the linear recovery curve of the GFP-tagged full-length moesin protein (Figure 22).

To determine what degree of evolutionary conservation can be observed in the CRS, we aligned the sequences of 21 FERM domain containing proteins found in 12 species using Clustal Omega. Based on the results of the alignment, it seems that a highly conserved region of 22 amino acids can be identified in all proteins examined. Out of the 22 amino acids, five are the same in all sequences analyzed, while 8 other positions are filled by amino acids with similar chemical properties and thus, they contribute to the high degree of conservation (Figure 23).

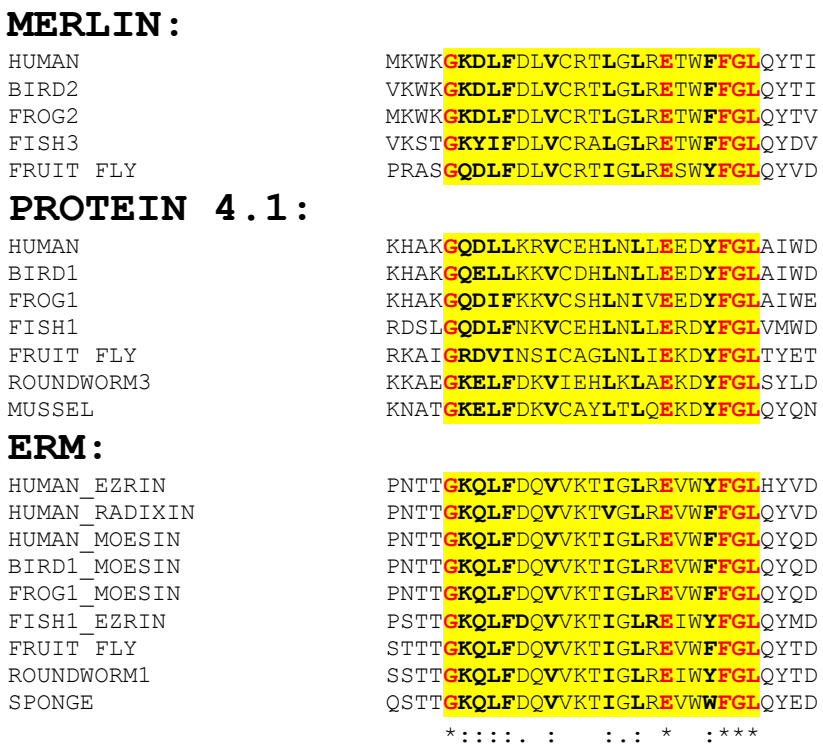

Figure 23. Multiple sequence alignment with Clustal Omega reveals that the CRS identified in the FERM domain of human Merlin extends to the Protein 4.1 and ERM families. Conserved CRS region is highlighted in yellow. Asterisks (*) and red letters indicate single, fully conserved residues, colon (:) and bold letters indicate conservation between groups of strongly similar properties, subscript period (.) indicates conservation between groups of weakly similar properties, no mark indicates no conservation. Species names and protein accession numbers can be found in Table 1. in the Appendices section.

This region contains the 12 amino acids that we referred to as “CoreCRS” in the previous experiments and roughly corresponds to the sequence which we named “CRS”. N-terminally to the evolutionary conserved region of 22 amino acids, our CRS sequence contained 3 additional threonines (Figure 24). Taken together, this short stretch of 22 amino acids identified by the sequence alignment shows a high degree of conservation across multiple species, indicating that the CRS might be indeed an important part of the FERM domain by playing a role in the regulation of the cellular localization of FERM domain-containing proteins.

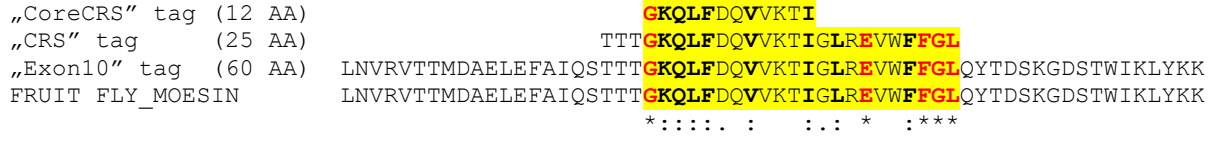

Figure 24. Comparison of the different CRS tags that were fused to GFP and their relation to the conserved part of the CRS sequence. Highlights and symbols are the same as those in Figure 23.

DISCUSSION

It has been known for some years that the actin-binding cytoskeletal protein, moesin is present not only in the cytoplasm, but also in the nucleus. Using two-dimensional electrophoresis and mass spectrometry, moesin was detected in the nuclei of human blood lymphocytes (Bergquist et al., 2001). Another study revealed that in human, all members of the ERM protein family, ezrin, radixin and moesin, localize to the nucleus (Batchelor et al., 2004). In the present dissertation, we investigated the dynamics and mechanisms by which moesin, the only member of the ERM protein family found in *Drosophila*, enters the nucleus.

First, using the nuclear FRAP method, we were able to reveal that moesin indeed shows nuclear import activity in interphase Drosophila S2R+ cells. However, the intensity is at a low level, suggesting that under normal, uninduced conditions, the nuclear import of moesin is strongly inhibited. This was an unexpected result for us. In a 2013 study, Johnson et al. investigated the nuclear import dynamics of two other actin-binding proteins using nuclear import FRAP assay. They found, that IQGAP1 and Rac1 both entered the nucleus with dynamics similar to that of actin (Johnson et al., 2013). Being an actin-binding protein, we expected similar import dynamics from moesin. The inhibition of mRNA export induced the accumulation of moesin in the nucleus and increased its nuclear import rate, revealing that the nuclear import of moesin is indeed an active, regulated process. However, even then, the intensity of the import was still quite different from that of a protein that is actively and dynamically transported into the cell nucleus.

Experiments carried out previously in our lab revealed that moesin utilizes a bipartite nuclear localization sequence ($KR_{X13}RRRK_{297}$) located on its N-terminal FERM domain to enter the nucleus. Examining the corresponding sequence of numerous ERM proteins from various species representing a wide range of evolutionary complexity, we found that the NLS motif of moesin we identified shows strong evolutionary conservation. Not only in terms of residues, but also in terms of the structure and the spacing between the two parts of the sequence.

Although we managed to determine the NLS sequence in Drosophila moesin, our experiments showed that moesin is present in the nucleus in small amounts, also in the complete absence of the motif. The most likely explanation for this is provided by previous live imaging experiments in our laboratory which showed that moesin binds to the chromosomes at the end of mitosis and enters the re-forming nucleus, and this process also occurs in the absence of the NLS (Vilmos et al., 2009). In addition, we also showed that most of the moesin proteins does

not leave the nucleus (Kristó et al., 2017). Under unstressed conditions, this relatively small amount of nuclear moesin is sufficient for its functions, and increased nuclear import is only necessary when transcription is elevated or nuclear mRNA export is blocked. Therefore, it is likely that unlike insect ERMs, mammalian ERMs use NLS2 for nuclear internalization following cell division, while the NLS1 we identified only functions under stress conditions. However, this is certainly not the case in *Drosophila*, as moesin engulfment into the nucleus can be observed even in the absence of NLS2, Moe-DNLS2 is clearly present in the nucleus after mitosis (Kovács et al., 2024).

In the literature we can find multiple cases, where the regulation of the NLS is facilitated by the phosphorylation of amino acids located in the vicinity of the NLS (Harreman et al., 2004; Nardozzi et al., 2010). In the case of moesin, two phosphorylatable amino acids, Y292 and T300 are located near the nuclear localization sequence. After replacing these residues with non-phosphorylatable and phosphomimetic amino acids, we examined whether these mutant proteins are able to accumulate in the nucleus after the induction of import. We found that all mutant variants accumulated in the nucleus upon *Rae1* RNAi treatment, demonstrating that they were imported into the nucleus and suggesting that in the case of Drosophila moesin, phosphorylation of the NLS region does not regulate import.

Since the phosphorylation status of the phosphorylatable amino acids near the NLS did not play a role in the regulation of the nuclear import of moesin, we tested another possibility. The moesin protein can have an inactive (closed) or active (open) conformation. In order for the protein to switch from the closed to the open arrangement, it must bind PIP2 and be phosphorylated at a threonine (T559) located at the C-terminus. To determine whether the closed or open conformation could be import-competent, we created MoeT559A (inactive) and MoeT559D (active) mutants. Examining nuclear import dynamics, subcellular localization and the ability to accumulate in the nucleus upon induction of import of these mutants, we found that although both mutant forms were able to enter and accumulate in the nucleus, the closed conformation seems to be preferred for nuclear import. This conclusion is further supported by the observations that the knockdown of Slik kinase alone, which is responsible for the phosphorylation of T559, increases the amount of nuclear moesin. In addition, the MoeKA mutant which has no PIP2 binding capacity and is therefore certainly in closed conformation, was shown to enter the nucleus just as well as the wild-type protein (result of Csaba Bajusz). Furthermore, our conclusion is consistent with that reported for the closest relative of the ERM proteins, merlin/NF2, showing that the closed form of merlin enters the nucleus (Li et al., 2010).

The constitutively active moesin mutant, MoeT559D failed to accumulate in the nucleus as much as its inactive counterpart, MoeT559A. The active state means that the general protein binding FERM domain of moesin does not interact with the C-terminal actin binding domain and is thus capable of recognizing and binding other proteins. If we examine the subcellular distribution of the active mutant form, MoeT559D, we can see that it preferentially localizes to the plasma membrane (Figure 12). This confirms that the protein is in fact active and binds partners at the cell cortex. Moreover, in its active state, moesin can bind partners not only through its N-terminal FERM-, but also with its C-terminal F-actin binding domain. To investigate whether F-actin binding is the reason why MoeT559D is not able to accumulate in the nucleus to such extent as MoeT559A, we increased or decreased the amount of intracellular F-actin in S2R+ cells with the help of the cytoskeletal drugs, Jasplakinolide and Latrunculin A, respectively. Neither treatments caused significant change in the amount of nuclear moesin, suggesting that F-actin binding is not preventing bulk amounts of moesin from moving into the nucleus. To further confirm this finding, we examined the capacity of nuclear accumulation upon induction of import of a moesin mutant that lacked its C-terminal domain, therefore it was incapable of F-actin binding. Since this mutant was not able to accumulate in the nucleus, our previous conclusion gained further support.

We found no evidence for the direct regulation of the NLS, and F-actin is also not responsible for the weak protein import observed, so it is evident that something else is holding the protein back in the cytosol. Since the mutants that cannot bind PIP2 (MoeKA) and are non-phosphorylatable at T559 (MoeT559A) both can enter the nucleus and accumulate there, it is reasonable to assume that moesin is held back in the cytoplasm by interactions of the FERM domain. This idea is supported by the previous observation that in the case of ezrin, association/dissociation with the membrane through the FERM domain is almost 10 times slower, i.e. stronger, than the interaction with F-actin (Fritzsche et al., 2014). However, the nuclear accumulation examined in our immunostaining experiments reflects an end state, it does not necessarily mean that the dynamics of import have changed. Therefore, we investigated the nuclear import dynamics of the inactive form, MoeT559A, which binds weakly with its FERM domain and therefore does not localize to the cortex, using FRAP. Surprisingly, we found that the protein can enter the cell nucleus in larger quantities, but with the very same weak dynamics as the wild-type protein which is inhibited by the supposed retention. This suggested us that binding partners of the FERM domain are not responsible for the retention, thus it must occur via a different mechanism.

In a close relative of the ERM proteins, merlin, which also has a FERM domain, Kressel and Schmucker were able to observe that the protein contains a sequence in its FERM domain which is responsible for cytoplasmic retention (Kressel and Schmucker, 2002). Since merlin shows a high degree of similarity to ERM proteins, we compared the sequence identified in merlin as responsible for cytoplasmic retention to the corresponding residues in moesin. The comparison revealed that there is a high degree of similarity between the two sequences. To test whether the sequence in moesin also functions as a CRS, we first created the MoeΔCRS mutant, in which we deleted part of the putative CRS, and conducted nuclear FRAP assays with it. The FRAP recovery curve corroborated our theory that moesin has a functional CRS sequence. To further confirm this result, we fused moesin CRS-containing moieties of various sizes to GFP, a protein that under normal conditions localizes to both the nucleus and the cytoplasm and is small enough to travel freely between the two cellular compartments. We found that two of the three peptides we tested, which we named "CRS" (25 amino acids) and "Exon10" (60 amino acids), were able to prevent GFP from entering the nucleus, even though the size of the tagged GFP proteins would allow diffusion through the NPC. This result was further confirmed by nuclear FRAP assays which showed that GFP tagged with the moesin CRS was essentially unable to traffic into the nucleus. We compared the corresponding sections of the CRS sequence of Drosophila moesin in several FERM domain-containing proteins of various species representing diverse phylogenetic taxa, and with the help of this we were able to determine that a stretch of 22 amino acids shows a high degree of evolutionary conservation. This conserved sequence corresponds almost precisely to the 25 amino acids long motif determined by us as "CRS". The conserved region of 22 amino acids can be divided into three clusters that are separated from each other by two to three non-conserved amino acids. It would be interesting to see, how the individual deletion/alanine substitutions of these smaller clusters influence the cytoplasmic retention of moesin.

In the future, we would like to further explore the cytoplasmic retention of moesin. Based on the results and information available we hypothesize that the identified CRS of moesin may be the binding site of an as yet unknown cytoplasmic factor that is itself anchored in the cytoplasm and that recognizes and binds moesin through the CRS sequence. As we have already shown that moesin accumulates in large quantities in the nucleus as a result of heat shock (Kristó et al., 2017) and regulates the transcription of heat shock genes (Bajusz et al., 2021), chaperone proteins are one of the obvious binding partner candidates. Considering that the NLS and CRS of moesin are spatially close to each other (Figure 25), it also raises the possibility

that the CRS-binding protein partner masks the NLS, making it unrecognizable for the importin of moesin. In order to test these and to identify the possible cytoplasmic binding partner, we plan to conduct a series of experiments. The first step would be to carry out co-immunoprecipitation with Exon10-GFP and GFP and then use mass spectrometry to identify the protein(s) that bind Exon10-GFP, but not GFP. Hopefully, this will provide a list of proteins that may be prime candidates for investigation of CRS binding partners responsible for the cytoplasmic retention of moesin.

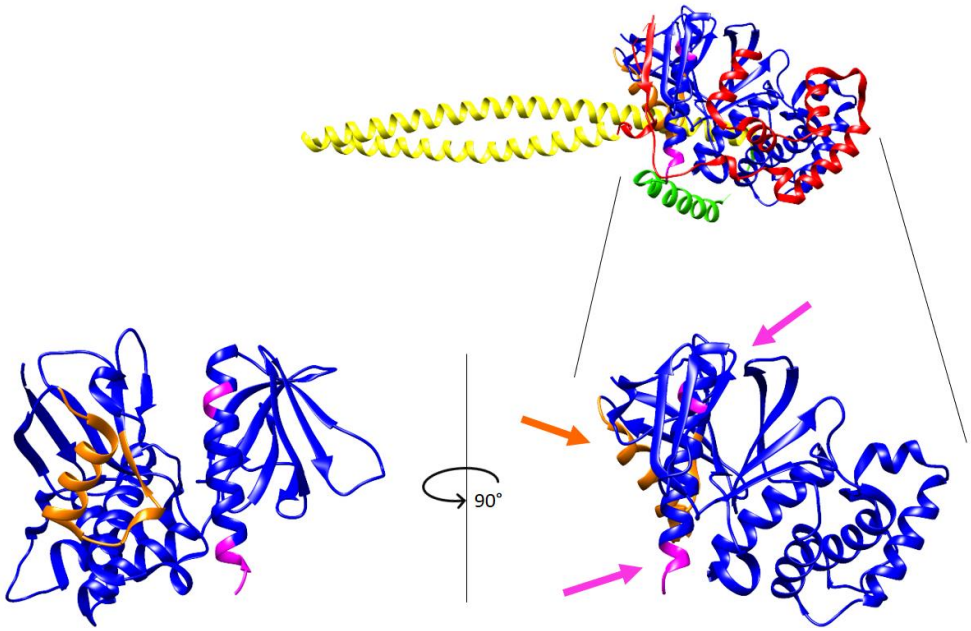

Figure 25. Location of the NLS (magenta) and the CRS (orange) of moesin in the folded protein.
Upper part: full length *Spodoptera frugiperda* moesin, closed conformation. FERM domain is highlighted in blue, the C-terminal domain is red. The alpha-helix connecting the two domains is shown in yellow. Green indicates a short alpha-helix connecting the FERM and the alpha-helical domains. (PDB ID: 2I1K).
Lower part: only the N-terminal FERM domain shown. Magenta arrows point toward the two parts of the bipartite NLS. Orange arrow indicates the CRS.

SUMMARY

The moesin protein of *Drosophila melanogaster*, which is primarily a cytoskeletal protein but is also present in the nucleus, uses a bipartite NLS sequence located in its N-terminal FERM domain to enter the nucleus. Because under normal conditions moesin's nuclear import is weak, but upon certain stimuli it can intensify, we believe that it is a tightly regulated, active process. One possible explanation for the weak baseline import would be that the activity of the NLS of moesin is somehow regulated. With our experiments, we were able to exclude phosphorylation of nearby amino acids as a possible mechanism for this. Further experiments revealed that the regulation of nuclear import by changing the conformational state does not mean strict regulation, although our data strongly suggest that the closed conformation is favored during nuclear translocation. Another possibility that F-actin binding is preventing moesin from moving into the nucleus, has also been disproven. Lastly, we were able to identify cytoplasmic retention as a major mechanism that plays a key role in keeping the nuclear level of moesin low.

Based on the findings presented in this dissertation, we can create a model of the regulation of the nuclear import of moesin (Figure 26). According to this, under uninduced conditions, moesin is primarily localized in the cytoplasm of interphase cells, because the protein's nuclear import is strongly suppressed. This suppression is achieved by multiple mechanisms working in cooperation. Firstly, when moesin is in its active, open conformation, it is mostly localized to the plasma membrane, fulfilling its classic, cytoplasmic role, that is, anchoring transmembrane proteins to the actin cytoskeleton. Then, even if moesin is in its closed conformation, which is preferred for nuclear entry, interaction with an as yet unknown cytoplasmic factor through the CRS sequence prevents nuclear import. However, in certain cases, such as for example increased transcriptional activity of the cell, which can be triggered by multiple effects such as hormone treatment, heat stress or the inhibition of mRNA export, moesin enters the nucleus, where its amount increases to relatively high levels (Kristó et al., 2017). Based on our results, this increased nuclear import activity is most likely caused by the release of moesin from the binding of the CRS-recognizing cytoplasmic factor as a result of stress, thereby making moesin's NLS accessible to its importin which finally transports moesin via the NPC into the nucleus.

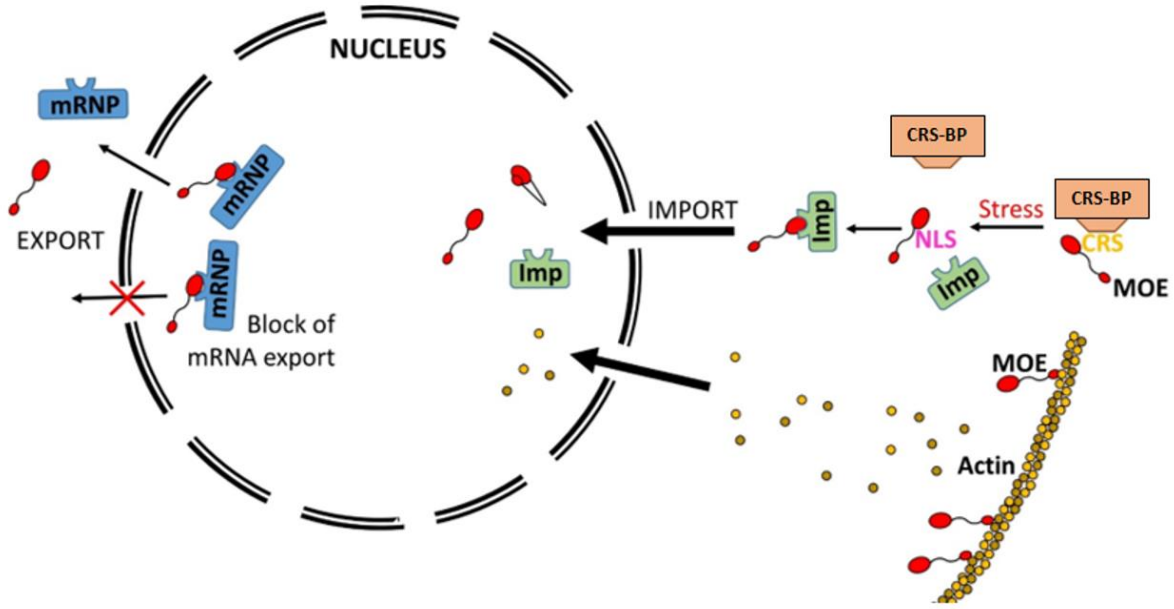

Figure 26. Model depicting the regulation of the subcellular localization of Drosophila moesin. MOE: moesin, CRS-BP: CRS binding protein, Imp: importin, NLS: nuclear localization signal, mRNP: messenger ribonucleoprotein, mRNA: messenger RNA.

FUNDING

This work was supported by NKFIH (Hungarian National Research, Development and Innovation Office) through the National Laboratory for Biotechnology program, grant 2022-2.1.1-NL-2022-00008.

ACKNOWLEDGEMENTS

I would like to express my deepest appreciation to my supervisor, Péter Vilmos for guiding me along the path leading up to this day. I am grateful for all the help he gave me throughout the years, both professionally and personally.

I'm extremely grateful to Ildikó Kristó, who was my mentor in the first years and who gave me strong foundations regarding lab work and scientific attitude. She was a great and invaluable example.

Many thanks to all current members of the Drosophila Nuclear Actin Laboratory, Ildikó Kristó, Péter Borkúti, Anikó Szabó, Csilla Abonyi, Réka Benke and Zsófia Pákai. I am also grateful to former members of the lab, especially Csaba Bajusz.

I would like to thank all current and former members of the Cellular Imaging Laboratory of the BRC, particularly Gábor Steinbach, Ildikó Valkonyné Kelemen and Ferhan Ayaydin, for helping in the planning and execution of various microscopic experiments.

I am grateful to Zoltán Hegedűs (BRC, Laboratory of Bioinformatics) and Gábor Steinbach (BRC, Cellular Imaging Laboratory) for their help in performing the statistical analyzes and evaluating the FRAP data presented in this dissertation, respectively.

Many thanks to Gábor "Melák" Csordás (BRC) and Zoltán Villányi (University of Szeged) for the critical reading of this dissertation.

This endeavor would not have been possible without the unconditional love and support of my family. I am especially grateful to my Mother, Erika Pintér and my Grandmother, Etelka Szalma, who always took the time and effort to study with me during my elementary and high school years.

APPENDICES

Table 1
Summary of the ERM protein sequences analyzed for evolutionary conservation, presented in Figures 10, 19, 23 and 24.

Organism	Scientific name	Common name	UniProt ID
Beetle	*Tribolium castaneum*	Red flour beetle	D6W9I6 (ERM1)
Bird1	*Gallus gallus*	Red junglefowl	A0A1D5NYK7 (moesin), A0A3Q2UBU1 (protein 4.1)
Bird2	*Meleagris gallopavo*	Wild turkey	G1NBZ6 (merlin)
Choanoflagellate	*Monosiga brevicollis*	-	A9URX5 (ERM-like)
Fish1	*Danio rerio*	Zebrafish	Q5TZG5 (ezrin), Q66I42 (moesin), Q8JG61 (protein 4.1)
Fish2	*Oryzias latipes*	Rice fish	A0A0D6A9B1 (moesin)
Fish3	*Esox lucius*	Northern pike	A0A6Q2XS73 (merlin)
Frog1	*Xenopus laevis*	African clawed frog	A0A1L8HAW1 (radixin), Q4V7Z2 (moesin), P11434 (protein 4.1)
Frog2	*Xenopus tropicalis*	Western clawed frog	Q0IIY8 (merlin)
Fruit fly	*Drosophila melanogaster*	Fruit fly	P46150 (moesin), X2JFU0 (merlin), Q9V8R9 (protein 4.1)
Human	*Homo sapiens*	Human	P15311 (ezrin), P35241 (radixin), P26038 (moesin), P35240 (merlin), P11171 (protein 4.1)
Hydra	*Hydra vulgaris*	Fresh-water polyp	T2MG47 (radixin)
Moth1	*Bombyx mori*	Silk moth	A0A8R1WN82 (ERM1)
Moth2	*Spodoptera frugiperda*	Fall armyworm	A0T1L9 (ERM1)
Mouse	*Mus musculus*	House mouse	P26040 (ezrin), P26043 (radixin), P26041 (moesin)
Mussel	*Mytilus edulis*	Blue mussel	A0A8S3SC82 (protein 4.1)
Roundworm1	*Caenorhabditis elegans*	-	G5EBK3 (ERM-1)
Roundworm2	*Caenorhabditis tropicalis*	-	A0A1I7V2T8 (ERM1)
Roundworm3	*Anisakis simplex*	Herring worm	A0A0M3JU72 (protein 4.1)
Sponge	*Amphimedon queenslandica*	-	A0A1X7V0F6 (FERM domain containing protein)
Starfish	*Acanthaster planci*	Crown-of-thorns starfish	A0A8B7ZPU5 (Radixin-like)
Tapeworm	*Echinococcus granulosus*	Hydatid worm	W6UQS2 (ERM)
Water bear	*Hypsibius dujardini*	-	A0A1W0WJ32 (ERM-like)

Appendix 2

Sequence of the template used in the *Slik* RNAi *in vitro* transcription reaction (yellow highlight: T7 promoter sequence)

5′ - TAATACGACTCACTATAGGGCTCCAGTCACCACGGCTATTGAGGTGGCCATTGGCCAAGAAGCG
ATGGAGCCCAAACCGCAGCCGCCATCGCCCACAGCCTCCTCCATTGTGTCTGTGCAATCGGTGGCCTC
TTCCAGCTCTTCGGGCAGTGTTTCAAATGCTGTTCTCAGCTCGAGCACTTCCCTTATTACCATCAACA
GCGATCCACCCACACCGCATCATCACCAACCGCTGCCACCTCAACCGCAGCACTTGATTTTGCCAAAC
AGCTTGGAGTCGGTGAGTCAGATAACAGTCGTGACCAGCACCCATCCGCCGGTAATCATCGACAACTC
GGTGATGCCACCGCAAAACGAGGTGATCATCGTATCCAATGATATGAACAAGAGCACTCACCTGCATG
AATCTTCGACGGACGATGATTTTCCATCGCTGGACGACAGTTTGGGTGATGCCACCACGCCGCCCCAC
AAGCAATCCTCAATGATATTGGCTGTTAATGAGCCAGCAGGTGTGGTTCCTGCTCCTCCGTCGCCCTA
TAGTGAGTCGTATTA - 3′

REFERENCES

Ali, R. H., and Khan, A. A. (2014). Tracing the evolution of FERM domain of Kindlins. *Mol. Phylogenet. Evol.* 80, 193–204. doi: 10.1016/j.ympev.2014.08.008.

Arenzana-Seisdedos, F., Turpin, P., Rodriguez, M., Thomas, D., Hay, R. T., Virelizier, J. L., et al. (1997). Nuclear localization of IκBα promotes active transport of NF-κB from the nucleus to the cytoplasm. *J. Cell Sci.* 110, 369–378. doi: 10.1242/jcs.110.3.369.

Baeuerle, P. A., and Baltimore, D. (1988). Activation of DNA-binding activity in an apparently cytoplasmic precursor of the NF-κB transcription factor. *Cell* 53, 211–217. doi: 10.1016/0092-8674(88)90382-0.

Bajusz, C., Kristó, I., Abonyi, C., Venit, T., Vedelek, V., Lukácsovich, T., et al. (2021). The nuclear activity of the actin-binding Moesin protein is necessary for gene expression in Drosophila. *FEBS J.* 288, 4812–4832. doi: 10.1111/FEBS.15779.

Batchelor, C. L., Woodward, A. M., and Crouch, D. H. (2004). Nuclear ERM (ezrin , radixin , moesin) proteins : regulation by cell density and nuclear import. 296, 208–222. doi: 10.1016/j.yexcr.2004.02.010.

Baum, D. A. (2015). A comparison of autogenous theories for the origin of eukaryotic cells. *Am. J. Bot.* 102, 1954–1965. doi: 10.3732/ajb.1500196.

Baum, D. A., and Baum, B. (2014). An inside-out origin for the eukaryotic cell. *BMC Biol.* 12, 1–22. doi: 10.1186/s12915-014-0076-2.

Ben-Aissa, K., Patino-Lopez, G., Belkina, N. V., Maniti, O., Rosales, T., Hao, J. J., et al. (2012). Activation of Moesin, a Protein That Links Actin Cytoskeleton to the Plasma Membrane, Occurs by Phosphatidylinositol 4,5-bisphosphate (PIP2) Binding Sequentially to Two Sites and Releasing an Autoinhibitory Linker. *J. Biol. Chem.* 287, 16311. doi: 10.1074/JBC.M111.304881.

Bergquist, J., Gobom, J., Blomberg, A., Roepstorff, P., and Ekman, R. (2001). Identification of nuclei associated proteins by 2D-gel electrophoresis and mass spectrometry. *J. Neurosci. Methods* 109, 3–11. doi: 10.1016/S0165-0270(01)00395-8.

Devos, D. P., Gräf, R., and Field, M. C. (2014). Evolution of the nucleus. *Curr. Opin. Cell Biol.* 28, 8–15. doi: 10.1016/j.ceb.2014.01.004.

Dopie, J., Skarp, K. P., Rajakylä, E. K., Tanhuanpää, K., and Vartiainen, M. K. (2012). Active maintenance of nuclear actin by importin 9 supports transcription. *Proc. Natl. Acad. Sci. U. S. A.* 109, E544–E552. doi: 10.1073/PNAS.1118880109/SUPPL_FILE/PNAS.1118880109_SI.PDF.

Fehon, R. G., McClatchey, A. I., and Bretscher, A. (2010). Organizing the cell cortex: The role of ERM proteins. *Nat. Rev. Mol. Cell Biol.* 11, 276–287. doi: 10.1038/nrm2866.

Fievet, B. T., Gautreau, A., Roy, C., Del Maestro, L., Mangeat, P., Louvard, D., et al. (2004). Phosphoinositide binding and phosphorylation act sequentially in the activation mechanism of ezrin. *J. Cell Biol.* 164, 653. doi: 10.1083/JCB.200307032.

Fornerod, M., Ohno, M., Yoshida, M., and Mattaj, I. W. (1997). CRM1 is an export receptor for leucine-rich nuclear export signals. *Cell* 90, 1051–1060. doi: 10.1016/S0092-8674(00)80371-2.

Fritzsche, M., Thorogate, R., and Charras, G. (2014). Quantitative analysis of ezrin turnover dynamics in the actin cortex. *Biophys. J.* 106, 343–353. doi: 10.1016/J.BPJ.2013.11.4499.

Fu, H., Subramanian, R. R., and Masters, S. C. (2000). 14-3-3 P ROTEINS : Structure , Function , and Regulation.

Harreman, M. T., Kline, T. M., Milford, H. G., Harben, M. B., Hodel, A. E., and Corbett, A. H. (2004). Regulation of Nuclear Import by Phosphorylation Adjacent to Nuclear Localization Signals *. 279, 20613–20621. doi: 10.1074/jbc.M401720200.

Hipfner, D. R., Keller, N., and Cohen, S. M. (2004). Slik Sterile-20 kinase regulates Moesin activity to promote epithelial integrity during tissue growth. *Genes Dev.* 18, 2243–2248. doi: 10.1101/GAD.303304.

Hung, M., and Link, W. (2011). Protein localization in disease and therapy. doi: 10.1242/jcs.089110.

Johnson, M. A., Sharma, M., Mok, M. T. S., and Henderson, B. R. (2013). Stimulation of in vivo nuclear transport dynamics of actin and its co-factors IQGAP1 and Rac1 in response to DNA replication stress. *Biochim. Biophys. Acta - Mol. Cell Res.* 1833, 2334–2347. doi: 10.1016/j.bbamcr.2013.06.002.

Kaffman, A., and O'Shea, E. K. (1999). Regulation of Nuclear Localization: A Key to a Door. 291–339.

Kaul, S. C., Kawai, R., Nomura, H., Mitsui, Y., Reddel, R. R., and Wadhwa, R. (1999). Identification of a 55-kDa ezrin-related protein that induces cytoskeletal changes and localizes to the nucleolus. *Exp. Cell Res.* 250, 51–61. doi: 10.1006/EXCR.1999.4491.

Kelpsch, D. J., and Tootle, T. L. (2018). Nuclear Actin: From Discovery to Function. *Anat. Rec.* 301, 1999–2013. doi: 10.1002/ar.23959.

Kovács, Z., Bajusz, C., Szabó, A., and Borkúti, P. (2024). A bipartite NLS motif mediates the nuclear import of Drosophila moesin. 9, 1–14. doi: 10.3389/fcell.2024.1206067.

Krawetz, R., and Kelly, G. M. (2008). Moesin signalling induces F9 teratocarcinoma cells to differentiate into primitive extraembryonic endoderm. *Cell. Signal.* 20, 163–175. doi: 10.1016/J.CELLSIG.2007.10.011.

Kressel, M., and Schmucker, B. (2002). Nucleocytoplasmic transfer of the NF2 tumor suppressor protein merlin is regulated by exon 2 and a CRM-1 dependent nuclear export signal in exon 15. *Hum. Mol. Genet.* 11, 2269–2278. doi: 10.1093/hmg/11.19.2269.

Kristó, I., Bajusz, C., Borsos, B. N., Pankotai, T., Dopie, J., Jankovics, F., et al. (2017). The actin binding cytoskeletal protein Moesin is involved in nuclear mRNA export. *Biochim. Biophys. Acta - Mol. Cell Res.* 1864, 1589–1604. doi: 10.1016/j.bbamcr.2017.05.020.

Li, W., You, L., Cooper, J., Schiavon, G., Pepe-Caprio, A., Zhou, L., et al. (2010). Merlin/NF2 Suppresses Tumorigenesis by Inhibiting the E3 Ubiquitin Ligase CRL4DCAF1 in the Nucleus. *Cell* 140, 477–490. doi: 10.1016/j.cell.2010.01.029.

Li, X., Shou, W., Kloc, M., Reddy, B. A., and E, D. (1994). Cytoplasmic Retention of Xenopus Nuclear Factor 7 before the Mid Blastula Transition Uses a Unique Anchoring Mechanism Involving a Retention Domain and Several Phosphorylation Sites. 124, 7–

17.

Lu, J., Wu, T., Zhang, B., Liu, S., Song, W., Qiao, J., et al. (2021). Types of nuclear localization signals and mechanisms of protein import into the nucleus. *Cell Commun. Signal.* 19, 1–10. doi: 10.1186/S12964-021-00741-Y/FIGURES/1.

Martin, W. (2005). Archaebacteria (Archaea) and the origin of the eukaryotic nucleus. *Curr. Opin. Microbiol.* 8, 630–637. doi: 10.1016/j.mib.2005.10.004.

Mattaj, I. W., and Englmeier, L. (1998). Nucleocytoplasmic transport: The soluble phase. *Annu. Rev. Biochem.* 67, 265–306. doi: 10.1146/annurev.biochem.67.1.265.

Melendez-Vasquez, C. V., Rios, J. C., Zanazzi, G., Lambert, S., Bretscher, A., and Salzer, J. L. (2001). Nodes of Ranvier form in association with ezrin-radixin-moesin (ERM)-positive Schwann cell processes. *Proc. Natl. Acad. Sci. U. S. A.* 98, 1235. doi: 10.1073/PNAS.98.3.1235.

Miralles, F., Posern, G., Zaromytidou, A. I., and Treisman, R. (2003). Actin dynamics control SRF activity by regulation of its coactivator MAL. *Cell* 113, 329–342. doi: 10.1016/S0092-8674(03)00278-2.

Molnar, C., and de Celis, J. F. (2006). Independent roles of Drosophila Moesin in imaginal disc morphogenesis and hedgehog signalling. *Mech. Dev.* 123, 337–351. doi: 10.1016/j.mod.2006.02.001.

Nakamura, F., Amieva, M. R., and Furthmayr, H. (1995). Phosphorylation of threonine 558 in the carboxyl-terminal actin-binding domain of moesin by thrombin activation of human platelets. *J. Biol. Chem.* 270, 31377–31385. doi: 10.1074/jbc.270.52.31377.

Nardozzi, J. D., Lott, K., and Cingolani, G. (2010). Phosphorylation meets nuclear import : a review. *Cell Commun. Signal.* 8, 32. doi: 10.1186/1478-811X-8-32.

Pennisi, E. (2004). The birth of the nucleus. *Science (80-.).* 305, 766–768. doi: 10.1126/science.305.5685.766.

Polosello, C., Delon, I., Valenti, P., Ferrer, P., and Payre, F. (2002). Dmoesin controls actin-based cell shape and polarity during Drosophila melanogaster oogenesis. *Nat. Cell Biol.* 4, 782–789. doi: 10.1038/NCB856.

Rothwarf, D. M., Zandi, E., Natoli, G., and Karin, M. (1998). IKK-γ is an essential regulatory subunit of the IκB kinase complex. *Nature* 395, 297–300. doi: 10.1038/26261.

Salichs, E., Ledda, A., Mularoni, L., Albà, M. M., and De La Luna, S. (2009). Genome-Wide analysis of histidine repeats reveals their role in the localization of human proteins to the nuclear speckles compartment. *PLoS Genet.* 5. doi: 10.1371/journal.pgen.1000397.

Schwarzerova, K., Bellinvia, E., and Martinek, J. (2019). Tubulin is actively exported from the nucleus through the Exportin1 / CRM1 pathway. doi: 10.1038/s41598-019-42056-6.

Shibasaki, F., Price, E. R., Milan, D., and McKeon, F. (1996). Role of kinases and the phosphatase calcineurin in the nuclear shuttling of transcription factor NF-AT4. *Nature* 382, 370–373.

Speck, O., Hughes, S. C., Noren, N. K., Kulikauskas, R. M., and Fehon, R. G. (2003). Moesin functions antagonistically to the Rho pathway to maintain epithelial integrity. *Nature*

421, 83–87. doi: 10.1038/nature01295.

Vilmos, P., Jankovics, F., Szathmári, M., Lukácsovich, T., Henn, L., and Erdélyi, M. (2009). Live imaging reveals that the Drosophila actin-binding ERM protein, moesin, co-localizes with the mitotic spindle. *Eur. J. Cell Biol.* 88, 609–619. doi: 10.1016/J.EJCB.2009.05.006.

Wang, R., and Brattain, M. G. (2007). The maximal size of protein to diffuse through the nuclear pore is larger than 60 kDa. *FEBS Lett.* 581, 3164–3170. doi: 10.1016/j.febslet.2007.05.082.

Weis, K. (1998). Importins and exportins: How to get in and out of the nucleus. *Trends Biochem. Sci.* 23, 185–189. doi: 10.1016/S0968-0004(98)01204-3.

Zhu, J., and McKeon, F. (1999). NF-AT activation requires suppression of Crm1-dependent export by calcineurin. *Nature* 398, 256–260. doi: 10.1038/18473.